BMC Plant Biology

RESEARCH

Open Access

Identification and functional analyses of drought stress resistance genes by transcriptomics of the Mongolian grassland plant *Chloris virgata*

Ganbayar Namuunaa[1], Baldorj Bujin[1], Ayumi Yamagami[1*], Byambajav Bolortuya[1], Shintaro Kawabata[1], Hirotaka Ogawa[1], Asaka Kanatani[2], Minami Shimizu[2], Anzu Minami[2,3], Keiichi Mochida[2,3,4,5], Takuya Miyakawa[1], Bekh-Ochir Davaapurev[6], Tadao Asami[7], Javzan Batkhuu[6] and Takeshi Nakano[1*]

Abstract

Background Mongolian grasslands, including the Gobi Desert, have been exposed to drought conditions with few rains. In such harsh environments, plants with highly resistant abilities against drought stress survive over long periods. We hypothesized that these plants could harbor novel and valuable genes for enhancing drought stress resistance.

Results In this study, we identified *Chloris virgata*, a Mongolian grassland plant with strong drought resistance. RNA-seq-based transcriptome analysis was performed to uncover genes associated with drought stress resistance in *C. virgata*. *De novo* transcriptome assembly revealed 25,469 protein-coding transcripts and 1,219 upregulated genes after 3- and 6-hr drought stress treatments. Analysis by homology search and Gene Ontology (GO) enrichment indicated that abscisic acid (ABA)- and drought stress-related GO terms were enriched. Among the highly induced genes, ten candidate cDNAs were selected and overexpressed in *Arabidopsis*. When subjected to drought stress, three of these genes conferred strong drought resistance in the transgenic plants. We named these genes Mongolian Grassland plant Drought-stress resistance genes 1, 2, and 3 (MGD1, MGD2, and MGD3). Gene expression analyses in the transformants suggested that MGD1, MGD2, and MGD3 may activate drought stress-related signalling pathways.

Conclusion This study highlighted the drought resistance of *C. virgata* and identified three novel genes that enhance drought stress resistance.

Keywords *Chloris virgata*, Drought stress resistance, RNA-seq, Transcriptome

*Correspondence:
Ayumi Yamagami
yamagami.ayumi.6s@kyoto-u.ac.jp
Takeshi Nakano
nakano.takeshi.6x@kyoto-u.ac.jp
Full list of author information is available at the end of the article

Background

Mongolia is located at more than 1500 m in elevation and features steppe grasslands, mountains, and deserts without oceans. Summer in the Mongolian grassland is short, with little rain, and the winter is cold, with temperatures less than −20°C. In particular, in the Gobi Desert area of Mongolia, the climate is highly continental and dry, and the annual rainfall is only 50 mm [1]. In the Mongolian grassland, only plants with rapid growth abilities to adapt to the short summer and drought stress resistance characteristics can survive under these severe conditions.

Climate change with global warming is a severe problem for human society. Abnormal climates reduce crop and vegetable production in agriculture and extend desert areas, accelerating climate instability in a vicious cycle. Drought stress affects plants at morphological, physiological, biochemical, and molecular levels. In *Arabidopsis thaliana* (hereafter *Arabidopsis*) and rice, drought stress has been shown to impair growth, photosynthesis, and reproductive processes, suggesting its broad impact across monocots and dicots [2–4].

Abscisic acid (ABA) is widely known for its critical role in plant drought defense mechanisms. Under drought conditions, the transcription of *NINECIS-EPOXYCAROTENOID DIOXYGENASE 3* (*NCED3*), a key gene that encodes the ABA biosynthesis enzyme, is significantly upregulated, leading to increased ABA accumulation [5]. This triggers the activation of ABA signalling pathways, which regulate processes such as stomatal closure and the expression of stress-responsive genes, including *RESPONSIVE TO DESICCATION 29B* (*RD29B*), thereby enhancing drought resistance [6, 7]. Besides these well-characterized ABA-dependent pathways, the existence of ABA-independent pathways is known. Notably, the transcription factor *DEHYDRATION-RESPONSIVE ELEMENT-BINDING 2A* (*DREB2A*) plays a pivotal role in enabling plants to withstand combined heat and drought stresses by activating a wide array of stress-responsive genes, thereby contributing to enhanced resistance under such adverse environmental conditions [8–10].

To unravel drought-stress mechanisms, transcriptomics, such as microarray and RNA-seq analyses, has become a pivotal tool, offering comprehensive insights into gene expression under water-limited conditions. Early studies in the 1990s isolated nine *Arabidopsis* cDNAs responsive to desiccation, including the RD29 family [11], which has since become a widely used drought stress marker [12]. Microarray analyses using *Arabidopsis* have provided valuable insights into highly drought-inducible genes [13] and tissue-specific drought-inducible genes in leaves and roots [14]. Among them, a salt-tolerant zinc finger protein (*STZ*), a transcription factor from the Cys2/His2-type (C2H2) family, is involved in the water-stress response, with transgenic plants overexpressing *STZ* showing improved drought resistance in *Arabidopsis* and cotton [15, 16]. Similarly, rice microarrays have identified drought-inducible genes, 10 of which have been proposed as potentially serving as markers for drought stress responses [17]. One such gene, *EID1-like F-box protein 3* (*EDL3*), has been shown to confer drought tolerance in *Arabidopsis* when overexpressed, with transgenic plants exhibiting improved resilience to water limitation compared to wild-type plants [18]. RNA sequencing (RNA-seq), a technique developed through next-generation sequencing (NGS) technologies, has been widely employed not only for experimental plants but also for underutilized wild plant species. For example, RNA-seq analyses of highly salt-resistance wild species such as *Sophora moorcroftiana* [19] and *Caragana korshinskii* [20] have yielded insights into their adaptive mechanisms under drought conditions. However, studies on Mongolian grassland species remain limited.

Our previous research demonstrated that *C. virgata* Dornogovi accession, a Mongolian grassland species, exhibits the fastest germination rate and significant regrowth potential compared to agricultural crops [21]. Its rapid growth likely facilitates adaptation to the short summers of Mongolian grasslands. Using *de novo* RNA-seq analysis, we identified 21,589 transcripts during the early growth stages of *C. virgata*. Given its growth in the arid Gobi Desert, we hypothesized that *C. virgata* also possesses strong drought resistance mechanisms. This study aimed to investigate the drought resistance of *C. virgata* and identify drought-inducible genes through RNA-seq analysis. The functional roles of candidate genes in drought stress resistance were further validated by transforming them into *Arabidopsis*.

Methods

Plant materials and growth conditions

C. virgata seeds were harvested from the native grassland of Dornogovi Province, Mongolia. The voucher specimens were deposited in the Plant Herbarium Library of the Laboratory of Plant Biotechnology, National University of Mongolia (voucher number: 17.29.01) and identified by Dr. Shagdar Dariimaa. Rice (*Oryza sativa* L. cv. Nipponbare) seeds were obtained from the National Agriculture and Food Research Organization (NARO), Japan. *Arabidopsis thaliana* ecotype Columbia seeds were purchased approximately 20 years ago from Lehle Seeds (USA), a widely recognized supplier of *Arabidopsis* seeds. Rice and *Arabidopsis* seeds have been maintained and propagated in our laboratory since acquisition. Wheat (*Triticum aestivum* L. cv. Norin 61) and oat (*Avena sativa* L. cv. Tochiyutaka) seeds were purchased

from a seed supplier, Kuragi Co., Ltd. (Japan) and SNOW BRAND SEED Co., Ltd. (Japan), respectively. The seeds of *C. virgata*, rice, wheat, and oat were sterilized in 5% sodium chloride and 0.07% Tween-20 for 20 minutes and rinsed three times with sterile water for 10 minutes. For *Arabidopsis*, seeds were sterilized in 70% ethanol with 0.5% Triton X-100 for 30 minutes, transferred to ethanol, and rinsed for 1 minute. Seeds were placed on filter paper to remove the residual ethanol. After sterilization, the seeds of *C. virgata*, rice, wheat, oat, and *Arabidopsis* were sown on ½ Murashige and Skoog (MS) basal (Duchefa Biochemie, Netherlands) plates containing 1.5% sucrose and 0.9% phytoagar (Duchefa Biochemie, Netherlands). After 2 days of incubation at 4°C in the dark, the seeds were incubated at 22°C with a 16-h light/8-h dark photoperiod for plant growth. The seedlings were moved to the soil and grown in the growth chamber at 22°C.

Physiological experiments

For the drought stress treatment of *C. virgata*, rice, wheat, and oat on soil, 7-day-old seedlings grown on ½ MS medium were transplanted into the soil and grown for 5 weeks with sufficient water. Then, plants on the soil were subjected to drought treatment by withholding water for 10 days and rewatering for 7 days. The data were taken after rewatering. For the mannitol treatment of *C. virgata*, rice, and oat, 7-day-old seedlings grown on ½ MS medium were transplanted to ½ MS medium supplemented with 0, 300, and 350 mM mannitol for 3 weeks [22], and then the fresh weight, shoot length, and chlorophyll contents were measured. For the dehydration treatment of *C. virgata* and *Arabidopsis*, 7- to 10-day-old seedlings grown on ½ MS medium were transferred to empty parafilm (dehydration treatment) or ½ MS medium (control) for the indicated times [23]. For the drought stress treatment of *Arabidopsis* plants in soil, 4-week-old plants were grown in soil with sufficient water, after which the plants were subjected to drought stress by water withholding for at least 2 weeks and then rewatered for 1–2 days. All the pots were placed in a growth chamber in a random order, and the position of each pot was randomly changed every day to avoid positional effects. The survival rate, chlorophyll content, and fresh weight were calculated after rewatering. Each experiment was repeated at least 3 times.

Chlorophyll content measurement

To measure the total chlorophyll content, the aboveground parts of the plants were homogenized in liquid nitrogen using a BEADS CRUSHER μT-01 (TAITEC, Japan), added to 10 mL of 80% v/v acetone, incubated on ice in the dark for 10 minutes, and centrifuged at 4°C for 10 minutes at 13,000 rpm. The chlorophyll content of the centrifuged supernatants was determined at 646.6, 663.6, and 750 nm using a UV/VIS spectrophotometer (Ultrospec 2100 Pro, USA) [24].

RNA extraction and qRT–PCR analysis

Total RNA was extracted from approximately 50 mg of plant tissue using an RNeasy Plant Mini Kit (Qiagen, Germany) according to the manufacturer's protocol. First-stand cDNA was synthesized from 0.5 μg of isolated RNA using a PrimeScript RT Reagent Kit (Takara, Japan), and the qRT–PCR was conducted following the instructions provided for the Thermal Cycler Dice Real Time System III with TB Green Premix ExTaqII (Takara, Japan) [25]. The primer pairs used for qRT-PCR are listed in Supporting Information Table S1.

RNA sequencing, library construction, and transcriptome assembly analysis

For RNA sequencing, 7-day-old *C. virgata* plants grown on ½ MS medium were transferred to empty parafilm or ½ MS medium for 3 hr and 6 hr for dehydration-treated and control samples, respectively. Shoots were collected for sampling, while roots were carefully removed. Total RNA was extracted from the plant samples using the abovementioned method. Three independent RNA samples were used as biological replicates. Approximately 1.5–2 μg of RNA was used for mRNA-Seq library construction with a NextFlex Rapid Directional RNA-seq Library Prep Kit (Perkin-Elmer, USA), and the libraries were sequenced by DNBSEQ-T7 (MGI, China). The raw read dataset was submitted to the DNA Data Bank of Japan Sequence Read Archive (DDJB SRA) under accession number PRJDB18577. The raw RNA-seq reads were trimmed using Trimmomatic (v0.39) with the following parameters: PE -threads 70 -phred33 SLIDINGWINDOW:4:15 LEADING:20 TRAILING:20 MINLEN:50. The quality-checked reads were then assembled *de novo* using Trinity (v2.8.5) with the default parameter settings. The assembled sequences were further processed to remove redundancy using the pcap module of PBSuite (v15.8.24) with the following parameters: autopcap -m 1900 -y 80 -t 80. Further clustering was performed with CD-HIT-EST (v4.8.1) with the following parameters: -T 50 -c 0.8 -d 50 -M 1500, selecting the longest sequence as the representative for each cluster. Transdecoder (v5.5.0) was employed to identify sequences with high coding potential. To evaluate the coding potential, BLASTp searches against the Swiss-Prot database (using BLAST v2.10.1+) and domain searches against the Pfam-A database (using HMMER v3.3.1) were conducted. The nonredundant set of transcripts with coding potential was used as a reference for estimating gene expression levels. Gene expression levels were quantified by mapping the

quality-checked reads to this reference set using Salmon (v1.9.0), and the read counts per transcript were then calculated to determine expression levels using the salmon quant function. For differential expression analysis, upregulated genes were defined as those whose absolute fold change was >1.5, and the p values of all the statistical tests were converted to adjusted p values of <0.05 in the DEseq2 package (version 1.40.2). A Venn diagram was constructed with the Gplots package (version 3.1.3), and GO enrichment analysis was performed with the ClusterProfiler package (version 4.8.1, based on *org.At.tair.db* annotation), and the results were visualized in the R studio environment (version 2023.09.0+463) [26].

Generation of transgenic *Arabidopsis* plants

To generate transgenic overexpression plants, the full-length coding regions of the target genes were amplified using the primer pairs described in Supporting Information Table S1. The amplified fragments were introduced into the pENTR^{TM}/D-TOPO vector (Invitrogen, Carlsbad, CA) and subsequently cloned in accordance with the Gateway strategy (Invitrogen) into the binary vector pGWB2 [27, 28] containing a *CaMV35S* promoter. To generate GFP transgenic plants, the amplified fragments were cloned and inserted into the pENTR^{TM}/D-TOPO vector and subsequently cloned in accordance with the Gateway strategy into the binary vector pGWB6 containing a *CaMV35S* promoter [27, 28]. The plasmid fusion constructs were subsequently transformed into *Arabidopsis* plants via *Agrobacterium tumefaciens* strain GV3101:pMP90 using the floral dip method [29]. Transgenic lines were screened on ½ MS medium supplemented with 25 mg/L hygromycin. T_3 homozygous plants were used for all the experiments.

Phylogenetic tree and multiple sequence alignment analysis

Based on the amino acid sequences of *MGD1*, *MGD2,* and *MGD3*, the homologous genes were searched via BLASTP, in which the NCBI reference protein (refseq_protein) and MpTak1_v5.1 [30] from MarpolBase were used. On the basis of amino acid length and identity, the genes with e values = $1e^{-16}$ or lower were determined to be *MGD1*, *MGD2,* and *MGD3* homologous genes among the candidate genes identified via BLASTP. The amino acid sequences of the *MGD1*, *MGD2,* and *MGD3* homologous genes were aligned using MAFFT [31], in which the "auto" setting was used. From the alignment data produced by MAFFT, a phylogenetic tree was generated in IQ-TREE [32], and the treefile obtained from IQ-TREE was modified using iTOL [33]. The results of the multiple sequence alignment were visualized in ESPript 3.0 [34].

Detection of subcellular localization

For subcellular localization, the root cells of 4-day-old *35Spro:GFP Arabidopsis* plants were observed. The fluorescence signals of the GFP transgenic plants were detected using a Zeiss LSM 700 confocal laser-scanning microscope (Zeiss, Germany).

Structure prediction analysis

Structure prediction for the protein sequences was carried out using AlphaFold3 [35], XtalPred [36], InterPro [37], deepTMHMM [38], TOPCONS [39], and SOSUI [40] servers. Predictions using AlphaFold3 were performed using high-performance computing resources to handle the extensive computational demands of the model. The quality of the predicted structure was assigned by the predicted local distance difference test (plDDT) score [41], which indicates prediction confidence in a model. Structures were further analysed and validated to ensure prediction reliability. Protein hydropathy analysis was conducted using the NovoPro server, a tool for assessing hydrophobicity and hydrophilicity across protein sequences, using its default settings [42]. The hydropathy profiles were measured and calculated by the Kyte-Doolittle scale [43]. The results were further analysed and interpreted to highlight key hydrophobic and hydrophilic regions.

Results

The Mongolian grassland plant *Chloris virgata* is highly resistant to drought stress

C. virgata has been reported to grow in the southernmost area of the Gobi Desert of Mongolia. This habitat of *C. virgata* suggests that this plant is able to resist the stress conditions in the Gobi Desert. Given that several stress conditions prevent plant growth in desert areas, we focused on drought stress conditions in comparison with high light, high temperature, and high salinity soil.

To analyse the drought stress resistance of the *C. virgata* Dornogobi accession [21], we subjected *C. virgata* to water-withholding treatment and compared with those of monocot crops, including rice, oat, and wheat (Fig. 1A). For the water-withholding treatment, 5-week-old plants were grown on soil with sufficient water and then exposed to drought stress by water-withholding for 10 days and rewatering for 7 days. *C. virgata* showed a significant drought stress-resistant phenotype with fresh and green leaves, whereas almost all the leaves of rice, oats, and wheat showed severe wilting shapes and brown leaf colours. After rewatering, only *C. virgata* recovered to produce more green leaves. But the growth and greening of the leaves in rice, oat, and wheat were limited.

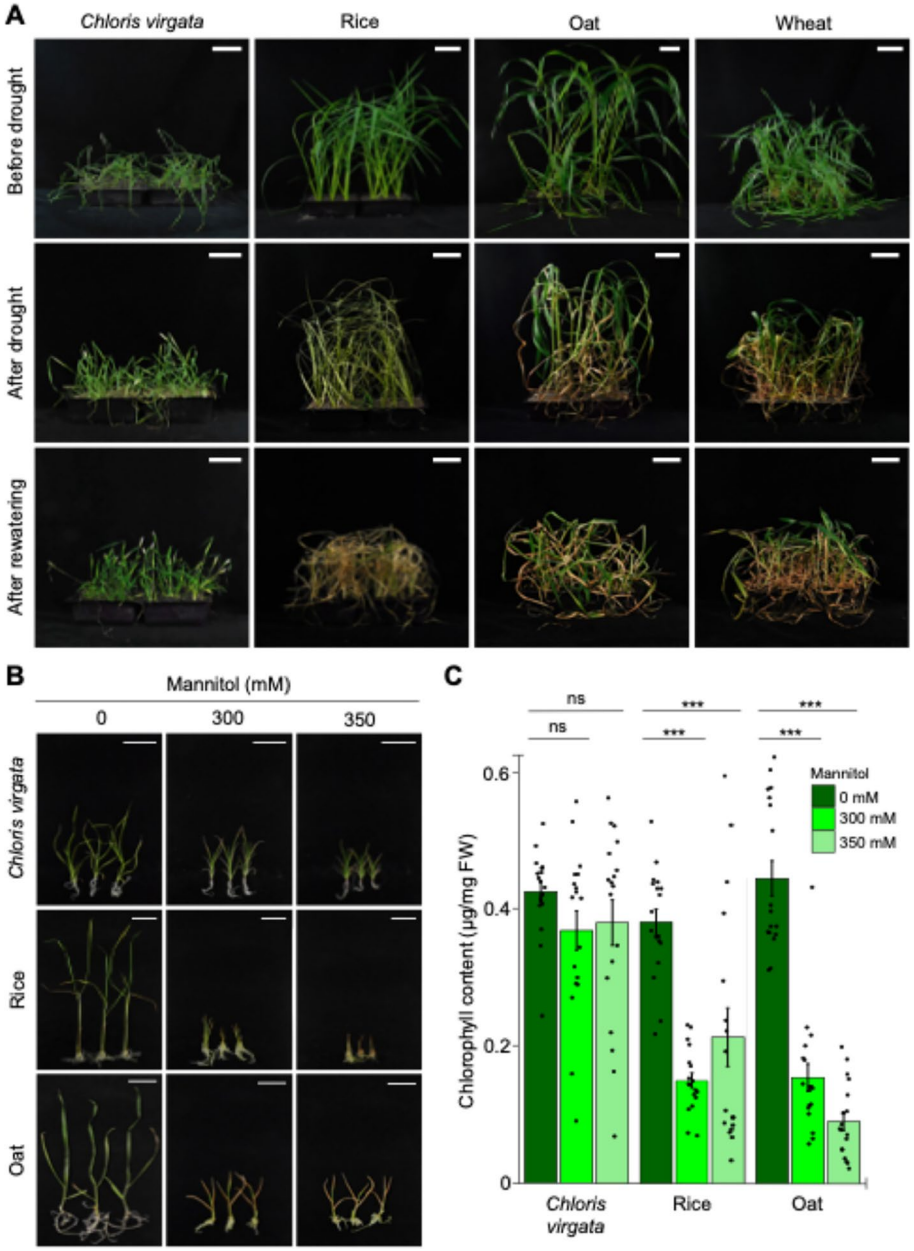

Fig. 1 *Chloris virgata* was resistant to drought stress. **A** Analysis of drought stress resistance in *Chloris virgata*, rice, oat, and wheat. Five-week-old plants were subjected to water-withholding treatment for 10 days, after which the plants were rewatered for 7 days. Scale bars = 10 cm. **B** Analysis of osmotic stress resistance in *Chloris virgata*, rice, and oat. Seven-day-old seedlings were subjected to mannitol treatment for 3 weeks at the indicated concentrations. Scale bars = 5 cm. **C** Endogenous chlorophyll contents of plants treated with mannitol. Statistical analyses were performed using Student's *t* test (ns = not significant, $^{***}P < 0.001$). n=18

As mannitol in plant growth medium is not absorbed by plants but takes over water from plants, mannitol is often used as an osmotic treatment that mimics drought stress conditions in plants [44]. To analyse the osmotic stress resistance of *C. virgata*, we applied high concentrations of mannitol to 7-day-old *C. virgata*, rice, and oat growing on ½ MS normal plates were transferred and grown on plates with high mannitol concentrations for 3 weeks. Because mannitol treatment affected plant greening (Fig. 1B), the total chlorophyll content was measured. In 300 mM and 350 mM mannitol media, the chlorophyll contents of rice and oat drastically decreased in comparison with those in the 0 mM control medium (Fig. 1C). Though

the growth of *C. virgata* was slightly inhibited by mannitol (Fig. S1), *C. virgata* maintained high endogenous chlorophyll contents in 300 mM and 350 mM mannitol media, which were similar to that of *C. virgata* on 0 mM control medium (Fig. 1C).

Drought stress-inducible gene expression in *Chloris virgata*

To explore the molecular function of *C. virgata* in drought stress resistance, the expression levels and expression periods of known drought-inducible genes in *C. virgata* were analysed (Fig. 2). Drought treatment was caused by the transfer of 7-day-old *C. virgata* from ½ MS plate to parafilm for 1 to 24 hrs. The *NCED3* gene encodes a 9-cis-epoxycarotenoid dioxygenase, a central enzyme in ABA biosynthesis [45, 46], and the overexpression of *NCED3* improved drought stress resistance to increase endogenous ABA contents and expression of drought- and ABA-inducible genes in *Arabidopsis*, rice, and soybean [5, 7, 47]. ABA-responsive element-binding protein 1 (*AREB1*) is a basic leucine zipper (bZIP) transcription factor that plays a central role in the ABA-dependent signalling pathway [48, 49], and the overexpression of *AREB1* has been shown to improve drought resistance in *Arabidopsis*, rice, and soybean [50–52]. In addition to the drought stress resistance activity, the early and precise inducibility of transcriptions of *NCED3* mRNA and *AREB1* mRNA were reported [5, 50]. Based on this knowledge, to determine the suitable stage for performing the *de novo* RNA-seq analysis of *C. virgata* under drought conditions, the *NCED3* and *AREB1/ABF2* genes were selected as drought-inducible marker genes [21]. The induction of *CvNCED3* mRNA expression started at 1 hr after drought treatment, and the most induced expression level was approximately 28-fold higher than that in non-drought-treated plants at 6 hr (Fig. 2A). *CvAREB1* expression was also induced at 1 hr and the most induced expression level was approximately 74-fold higher in the drought-treated plants than in the control plants at 6 hr (Fig. 2B). The gene expression levels of both *CvNCED3* and *CvAREB1* were decreased at 12 hr after drought treatment. In previous reports for *Arabidopsis*, the strong induction of *AtNCED3* [5] and *AtAREB1* [50] expression continued until 24 hr after drought treatment. The period to reach the maximum induction level of *CvNCED3* and *CvAREB1* might be earlier in *C. virgata* than in *Arabidopsis*.

De novo transcriptome assembly of drought-treated *Chloris virgata*

To analyse the detailed molecular mechanism of drought stress resistance in *C. virgata* and search for key genes that caused the drought stress resistance of *C. virgata,* we performed *de novo* RNA-seq analysis. Total RNA samples extracted from 3 hr and 6 hr dehydrated and untreated samples of *C. virgata* were pooled and subjected to RNA sequencing and *de novo* transcriptome assembly. A total of 1,307,170,602 raw sequence reads were generated from the *C. virgata* cDNA, and 1,281,678,077 were filtered reads. The quality-checked reads were assembled *de novo* using Trinity [53], resulting in 256,330 contigs with an N50 value of 2,366 bp. These contigs were assembled into 46,628 supercontigs with an N50 value of 2,723 bp by the

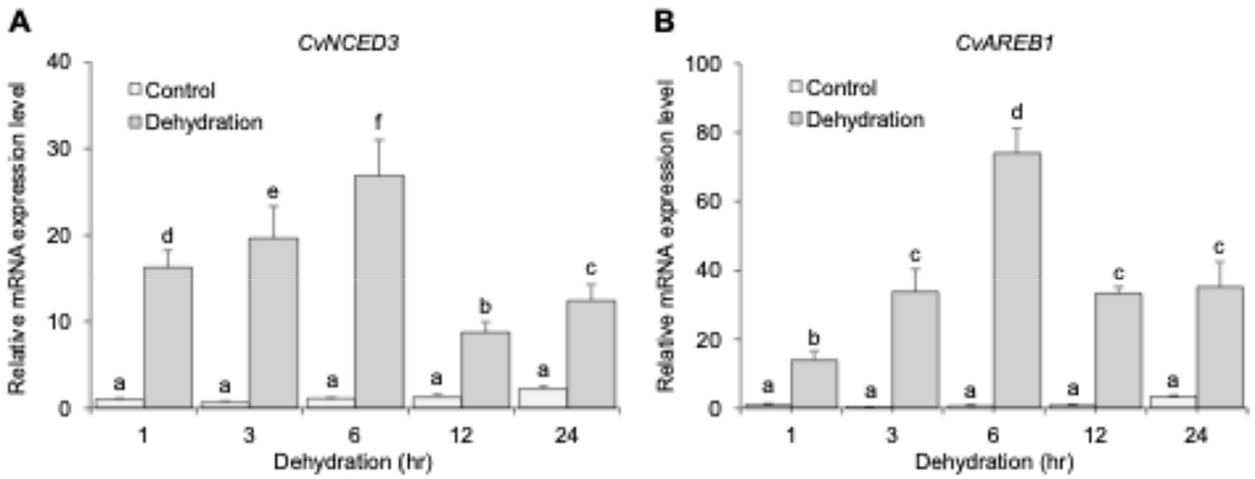

Fig. 2 Stress-inducible genes were highly expressed after drought treatment for 3 hr and 6 hr. **A**, **B** Expression levels of the *CvNCED3* (**A**) and *CvAREB1* (**B**) genes in *Chloris virgata* under dehydration stress. Seven-day-old plants were subjected to dehydration treatment or not for the indicated times. The relative expression levels were presented as an *n*-fold change compared with the value of the control treatment at 1 hr, which was set to 1. The error bars represent the means ± SDs from four replicated samples. The different letters above the bars indicate that the means are significantly different (One-way ANOVA with post-hoc Tukey HSD test ($P < 0.05$))

PCAP tool [54] and clustered using the CD-HIT-EST tool [55], resulting in 31,149 transcript clusters with an N50 value of 2,681 bp. The longest transcripts of the clusters were then subjected to open reading frames, resulting in the identification of 25,469 protein-coding transcripts, which were used in our downstream analysis as the reference transcript dataset. Among the reference transcripts, 22,683 (89%) and 21,501 (84%) were homologous to protein-coding genes in *O. sativa* (rice) and *Arabidopsis*, respectively, suggesting high reliability and completeness of the gene assembly in RNA-seq (Table S2). The Principal Component Analysis (PCA) revealed a distinct distribution in gene expression profiles between control samples (3 hr and 6 hr) and drought-treated samples (3 hr and 6 hr), indicating that drought treatment induces significant changes in gene expression compared to the control. Additionally, drought-treated samples from both time points (3 hr and 6 hr) exhibited a clear distribution, suggesting that the time-dependent response to drought stress strongly influences the gene expression profiles (Fig. S2).

Functional annotation of genes expressed at the drought-treated stage in *Chloris virgata*

To analyse the possible gene character of upregulated genes identified in the drought-treated RNA-seq analysis of *C. virgata*, the reference transcripts derived from the transcriptome assembly of *C. virgata* were assessed using a homology search and Gene Ontology (GO) enrichment. The homology search was conducted against the NCBI nonredundant database for the reference transcripts using the BLASTx program, and the highest hits were linked to the reference transcripts. The data were further subjected to GO enrichment analysis, and upregulated genes were identified with an adjusted p-value (padj) <0.05 and an absolute value of fold change >1.5 as the threshold at 3 hr and/or 6 hr of drought treatment. Compared with those in the control treatment, 1,182 and 1,198 genes were highly expressed at 3 hr and 6 hr, respectively. Among them, 1161 upregulated genes overlapped between 3 hr and 6 hr (Fig. 3A).

For a detailed analysis of the expressed genes, we divided these expressed genes into three clusters: genes whose expression was relatively high at the early stage after drought treatment for 3 hr rather than 6 hr (cluster 1, 21 upregulated genes), genes whose expression was relatively high at 6 hr rather than 3 hr (cluster 2, 37 upregulated genes), and genes whose expression was continuously expressed from 3 hr to 6 hr (cluster 3, 1161 upregulated genes) (Fig. 3A). By GO enrichment analysis of upregulated genes, a total of 139 and 2 GO terms were annotated in Cluster 3 and 1, respectively. However, in Cluster 2, no GO terms were annotated because

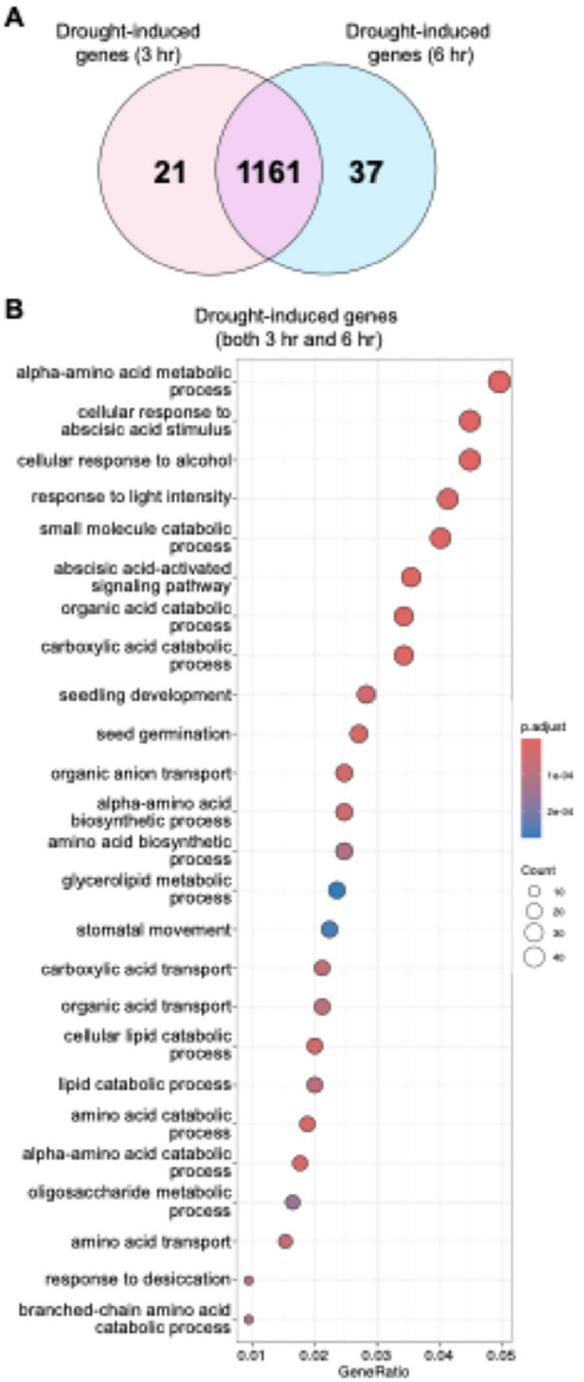

Fig. 3 Gene Ontology (GO) analysis of drought stress in *Chloris virgata*. **A** Venn diagram showing the upregulated genes ($P < 0.05$, fold change > 1.5) in *Chloris virgata* after dehydration for 3 hr and 6 hr. **B** Enrichment of GO annotations in biological process categories for genes upregulated after treatment with both 3 hr and 6 hr of dehydration. The y-axis indicates the pathway name, and the x-axis indicates the gene ratio. The p-adjusted value is represented by the colour of each dot, and the number of DEGs is represented by the size of each dot

of the small number of genes identified. We identified and listed the top 25 GO terms with the highest enrichment numbers in Cluster 3 (Fig. 3B). In the category of continuously drought-inducible genes for 3 hr and 6 hr grouped as Cluster 3, several enriched GO terms related to ABA pathways and direct drought stress response, such as 'cellular response to ABA stimulus', 'abscisic acid-activated signalling pathway', 'seed germination', 'stomatal movement', and 'response to desiccation', were identified. Many studies have shown that ABA is produced under drought stress conditions and plays an important role in the drought stress resistance of plants [56]. Moreover, embryonic ABA plays a central role in the induction and maintenance of seed dormancy and represses seed germination [57]. Stomatal closure via ABA promotes plant defense against drought stress by reducing transportational water loss in leaves. Therefore, ABA might be highly regulated at 3 hr and 6 hr of drought treatment during the desiccation resistance phase [58, 59].

To determine the drought effect occurred stage, we selected *CvNCED3* and *CvAREB1* as drought-inducible marker genes (Fig. 2). In the RNA-seq analysis, the log2 fold change of the *CvNCED3* (ChlorisST40659) gene was 4.11 for 3 hr and 4.41 for 6 hr drought treatment, whereas the log2 fold change of the *CvAREB1* (ChlorisST30712) was 2.20 for 3 hr and 2.41 for 6 hr drought treatment (Tables S3, S4). The result showed that the experimental procedure of the drought treatment for *C. virgata* and RNA-seq was successfully performed.

Moreover, we performed the GO analysis of downregulated genes (adjusted p-value < 0.05, fold change < −1.5) by dividing them into three clusters: genes whose expression was relatively low after drought treatment for 3 hr rather than 6 hr (cluster 1, 36 downregulated genes), genes whose expression was relatively low after drought treatment for 6 hr rather than 3 hr (cluster 2, 81 downregulated genes), and genes whose expression was continuously expressed from 3 hr to 6 hr (cluster 3, 558 downregulated genes) (Fig. S3). Due to the few gene identifications, only three GO terms were annotated in Cluster 1, including the 'plant-type cell wall cellulose metabolic process,' 'cell wall beta-glucan metabolic process,' and 'regulation of seed development.' A total of 25 and 17 GO terms are annotated in Cluster 2 and Cluster 3, respectively. GO enrichment analysis of downregulated genes in Cluster 2 were heavily implicated in ribosomal-related processes such as 'ribosome biogenesis,' 'ribonucleoprotein complex biogenesis,' 'ribosome assembly,' 'ribonucleoprotein complex assembly,' 'ribonucleoprotein complex subunit organization,' 'ribosomal small subunit assembly,' 'ribosomal large subunit biogenesis,' and 'ribosomal large subunit assembly.' Moreover, GO ontology analysis revealed that downregulated genes in Cluster 3 were found in growth-related processes, such as various kinds of cellular and metabolic processes. These results suggested that basic biological processes such as protein synthesis and cell wall synthesis would be inhibited in *C. virgata* under drought-stress conditions.

For all 25,469 ORFs of *C. virgata* predicted by *de novo* RNA-seq analysis, we compared the expression level of each gene in dehydration-treated plants with that in nondehydration-treated plants, and the induction ratios of all genes were ranked on the list. The highest log2 fold change values were identified as approximately 22- to 7-log2 fold change for the 60 genes identified after 3 hr of dehydration treatment and as approximately 30- to 10-log2 fold change for the 60 genes identified after 6 hr of dehydration treatment. The highest expression-increased top 60 genes of *C. virgata* after dehydration treatment for 3 hr and 6 hr in comparison with water-treated conditions are shown in Tables S3 and S4. The highest expression-suppressed top 60 genes are shown in Tables S5 and S6.

CvNCED3- and *CvAREB1*-overexpressing plants showed a drought stress-resistant phenotype

To confirm the technical possibility of the genetic manipulation of *Arabidopsis* by *C. virgata* genes and to analyse the functions of *C. virgata* homologues of drought-inducible and drought stress resistance genes in *Arabidopsis*, stress-inducible and stress resistance genes were transformed into *Arabidopsis*. The *CvNCED3* and *CvAREB1* cDNAs were fused under the cauliflower mosaic virus *35S* promoter (*CaMV35Spro*) and the constructed vectors were subsequently transformed into wild-type *Arabidopsis* using the *Agrobacterium* system. The expression of transgenes was analysed by qRT–PCR in transgenic *Arabidopsis* plants (Fig. S4A, B). As shown in Figure 2, *CvNCED3* and *CvAREB1* gene expression levels were highly induced at 3 hr and 6 hr after dehydration. The overexpression of *Arabidopsis NCED3* (*AtNCED3*) and rice *NCED3* (*OsNCED3*) resulted in drought stress resistance [5, 6]. Furthermore, modified *AtAREB1*- and intact *OsAREB1*-overexpressing plants also exhibited drought stress resistance [50, 60].

Transgenic and WT *Arabidopsis* plants grown under normal conditions with water in the soil for 4 weeks were exposed to drought stress by withholding water for 2 weeks and rewatering for 2 days. The results revealed that, after drought treatment, the WT rosette leaves turned yellow and wilted, and some of them died. Compared with the brown or yellow leaves of the WT plants, the *CvNCED3*- and *CvAREB1*-overexpressing plants presented relatively green and fresh rosette leaves. After rewatering, 67–75% of the *CvNCED3*-overexpressing plants and 100% of the *CvAREB1*-overexpressing plants

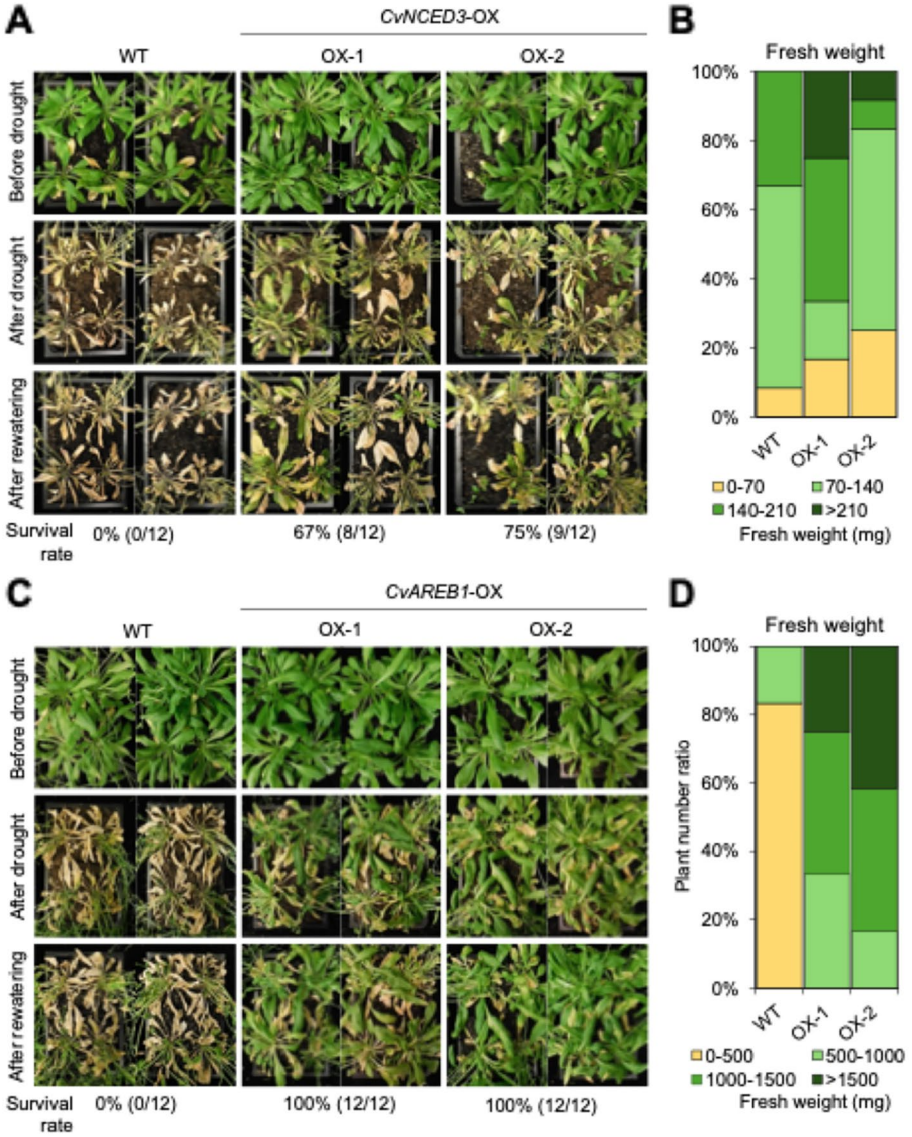

Fig. 4 *CvNCED3* and *CvAREB1* promoted drought stress resistance in *Arabidopsis*. **A**, **B** Survival rates (A) and fresh weights (B) of wild-type and *CvNCED3-OX Arabidopsis* plants under drought stress conditions. **C**, **D** Survival rates (**C**) and fresh weights (**D**) of wild-type and *CvAREB1-OX Arabidopsis* plants under drought stress conditions. Four-week-old plants were subjected to drought treatment for 14 days and then rewatered for 2 days. Survival rates were calculated from the number of living plants after 2 days of rewatering (n=12). The fresh weights were measured after 2 days of rewatering (n=12)

survived, whereas 0% of the WT plants survived (Fig. 4A, C). According to the results of the quantitative analysis, the ratio of plants with more than 210 mg of fresh weight was significantly higher in *CvNCED3*-overexpressing plants than in wild-type plants (Fig. 4B), whereas the ratio of plants showing more than 500 mg of fresh weight was higher in *CvAREB1*-overexpressing plants compared to wild-type plants (Fig. 4D), indicating that the overexpression of *CvNCED3* and *CvAREB1* can increase drought stress resistance in *Arabidopsis*. These results suggested that our experimental procedure to analyse the drought-stress resistance for *C. virgata* cDNA overexpressed *Arabidopsis* would be useful.

MGD1-overexpressing *Arabidopsis* plants showed greater drought stress resistance than did WT plants

To identify a novel gene that contributes to increasing the drought stress resistance of *C. virgata*, at first, we listed *C. virgata* cDNAs from the 60 highest induced genes in about 20,000 kinds of genes identified by *de*

novo RNA-seq after 3 hr and 6 hr of drought treatment (Tables S3, S4). As the drought-inducible marker genes *CvNCED3* and *CvAREB1* were lower and out of the top 60 genes, the listed 60 genes were considered more highly inducible than the well-known *NCED3* and *AREB1*. As we would like to identify the signalling factors related to drought-stress regulation, proteins whose possible localizations were predicted to be in the nuclear, cytosol, endoplasmic reticulum, Golgi, and plasma membrane were selected at first. Second, we would also like to identify novel factors related to drought-stress regulation, proteins whose detailed functions to increase drought-stress resistance had been reported elsewhere, e.g., *RD29B*, *DHN*, and others, being excluded from the list. Third, we would like to focus on protein signalling rather than the metabolic regulation of drought-stress resistance; possible enzyme proteins were also excluded. Based on the three rules for selection, ten genes that we considered novel and signalling protein candidates in the top 60 induced cDNAs of *C. virgata* are listed and highlighted in Tables S3 and S4.

These selected *C. virgata* cDNAs were fused under the *CaMV35S* promoter, and the constructed vectors were subsequently transformed into wild-type *Arabidopsis*. The T_3 generation of transgenic *Arabidopsis* with *C. virgata* cDNA was exposed to drought stress by withholding water from the plants, and the drought stress resistance of each transformant was observed.

Among all the selected *C. virgata* cDNAs, we initially focused on *ChlorisST30368* cDNA, because the cDNA finally showed the highest drought stress resistance. *ChlorisST30368* cDNA expression was approximately 7-fold greater after 3 hr of dehydration treatment and approximately 12-fold greater after 6 hr of dehydration treatment than in the control plants (Fig. 5A). *ChlorisST30368* encodes a novel gene that is conserved in homologous genes from various kinds of land plants, but an analysis of the detailed functions of these genes has not yet been reported (Fig. 5B).

To determine the drought stress resistance of *ChlorisST30368*, two independent overexpression lines (OX-1 and OX-2) were analysed in comparison with WT plants. qRT-PCR revealed that the transgene expression levels of *ChlorisST30368* in both transgenic lines were significantly higher (Fig. S4C). When *ChlorisST30368*-overexpressing *Arabidopsis* plants were grown on soil for 4 weeks with moderate water feeding, the leaf phenotypes of the transgenic lines and WT plants looked similar to each other (Fig. 5C). Compared with the WT plants, the overexpressing plants presented a significantly more resistant phenotype with fewer wilted leaves after the water withholding treatment for 2 weeks. After rewatering for 2 days, almost all of the WT plant leaves were wilted, and plant growth was limited; in contrast, the plants overexpressing *ChlorisST30368* were recovered with green and fresh leaves. The survival rates of the transgenic OX-1 and OX-2 lines were 75% and 100%, respectively, whereas the WT plants presented a 0% survival rate. Moreover, *ChlorisST30368*-overexpressing plants showed higher fresh weights than WT plants did after rewatering (Fig. 5D). These results suggest that the *ChlorisST30368* gene promotes drought stress resistance in *Arabidopsis*. We named the *ChlorisST30368* gene Mongolian Grassland plant Drought-stress resistance gene 1 (MGD1).

MGD1 encodes a functionally uncharacterized coiled-coil protein

The MGD1 protein contains 283 amino acids. Sequence alignment analysis revealed that the MGD1 protein was highly similar to homologues from monocot species, such as *T. aestivum* (XP_044345791.1, 64.78%), *O. sativa* (XP_015622376.1, 64.35%) and *B. distachyon* (XP_003567507.1, 63.53%). The similarities with proteins from dicot species, such as *N. tabacum* (XP_016510532.1, 50.81%) and *Arabidopsis* (NP_001330291.1, 48.91%), were lower than those with proteins from monocot species. The homologous gene in *Arabidopsis* (NP_001330291.1, AT5G45310) encodes an uncharacterized coiled-coil protein. Some studies have mentioned the AT5G45310 protein; for example, MIR169 microRNA was cloned 0.5 kb downstream of AT5G45310 [61], and a genetic locus similar to this gene was found in the A1 genome of *Brassica juncea* [62]. However, the detailed characterization of its molecular function and response to environmental stress has remained unclear.

Analysis of the evolutionary inheritance of structural motifs of proteins that are conserved across various species is important for investigating protein function. The coiled-coil is a prevalent structural motif that is found in approximately 10% of eukaryotic proteins [63] and consists of a heptad amino acid repeat (abcdefg), where the first (a) and fourth (d) positions are hydrophobic residues such as leucine (L), isoleucine (I), methionine (M), alanine (A), and valine (V) [64]. This sequence pattern facilitates the formation of an amphiphilic α-helix that engages via hydrophobic interfaces in a knob-to-hole packaging arrangement [65], forming a coiled-coil superhelix. Moreover, the coiled-coil regions of the MGD1 protein were predicted between approximately 56 to 128 amino acids by the XtalPred [36] and InterPro [37] servers and are highly conserved between monocot and dicot species (Fig. 6A, represented as a green line). According to the AlphaFold3 server, the MGD1 protein comprises one long α-helix structure at the N-terminus and three short α-helix structures at the C-terminus

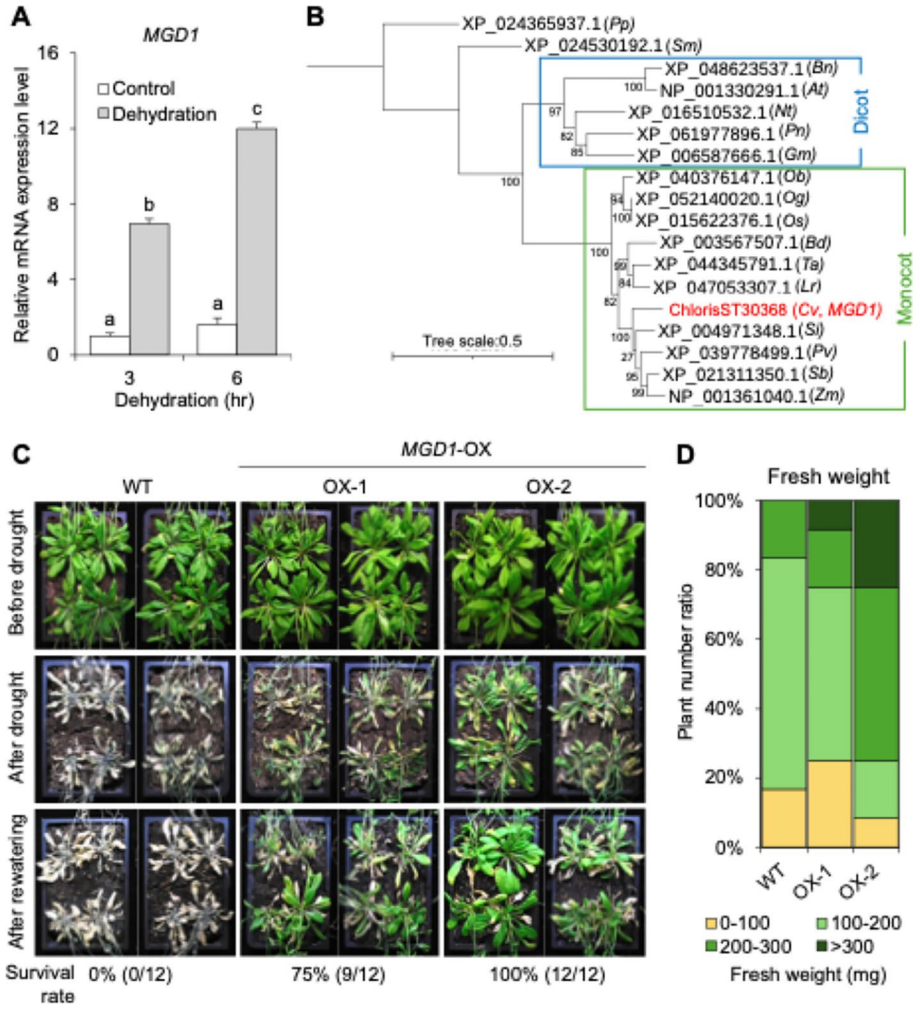

Fig. 5 *MGD1* promoted drought stress resistance in *Arabidopsis*. **A** Expression levels of the *MGD1* gene under dehydration stress in *Chloris virgata*. Seven-day-old plants were subjected to dehydration treatment or not for the indicated times. The error bars represent the means ± SDs from four replicated samples. The different letters above the bars indicate that the means are significantly different (One-way ANOVA with post-hoc Tukey HSD test ($P < 0.05$)). **B** Phylogenetic tree of MGD1 and related proteins in other species (*Pp, Physcomitrium patens; Sm, Selaginella moellendorffii; Bn, Brassica napus; At, Arabidopsis thaliana; Nt, Nicotiana tabacum; Pn, Populus nigra; Gm, Glycine max; Ob, Oryza brachyantha; Og, Oryza glaberrima; Os, Oryza sativa; Bd, Brachypodium distachyon; Ta, Triticum aestivum; Lr, Lolium rigidum; Cv, Chloris virgata; Si, Setaria italica; Pv, Panicum virgatum; Sb, Sorghum bicolor; Zm, Zea mays*). The numbers at the branching sites indicate the posterior probability values for nodal support. **C**, **D** Survival rates (**C**) and fresh weights (**D**) of wild-type and *MGD1-OX Arabidopsis* plants under drought stress conditions. Four-week-old plants were subjected to drought treatment for 14 days and then rewatered for 2 days. Survival rates were calculated from the number of living plants after 2 days of rewatering (n=12). The fresh weights were measured after 2 days of rewatering (n=12)

(Fig. S5B, Fig. 6A, represented as black lines). In addition, one possible transmembrane region was predicted in the N-terminus (Fig. 6A, represented as blue lines) by the deepTMHMM [38] and TOPCONS [39] servers. The predicted transmembrane region corresponded to and overlapped with the α-helix structure, whose region was predicted with high confidence (pIDDT score over 70), and with the hydrophobic regions of MGD1 (Fig. S5A, B). Using the AlphaFold3 server, we also modelled the MGD1 dimer, the results of which suggested that the coiled-coil region functions as a dimer interface to form a coiled-coil superhelix between two MGD1 molecules (Fig. S5C). This predicted structural information suggested that MGD1 might be an uncharacterized coiled-coil protein with one possible transmembrane helix.

To determine the subcellular localization of the MGD1 protein, transgenic *Arabidopsis* expressing the MGD1 protein fused to GREEN FLOURESCENT PROTEIN (GFP) driven by the *CaMV35S* promoter

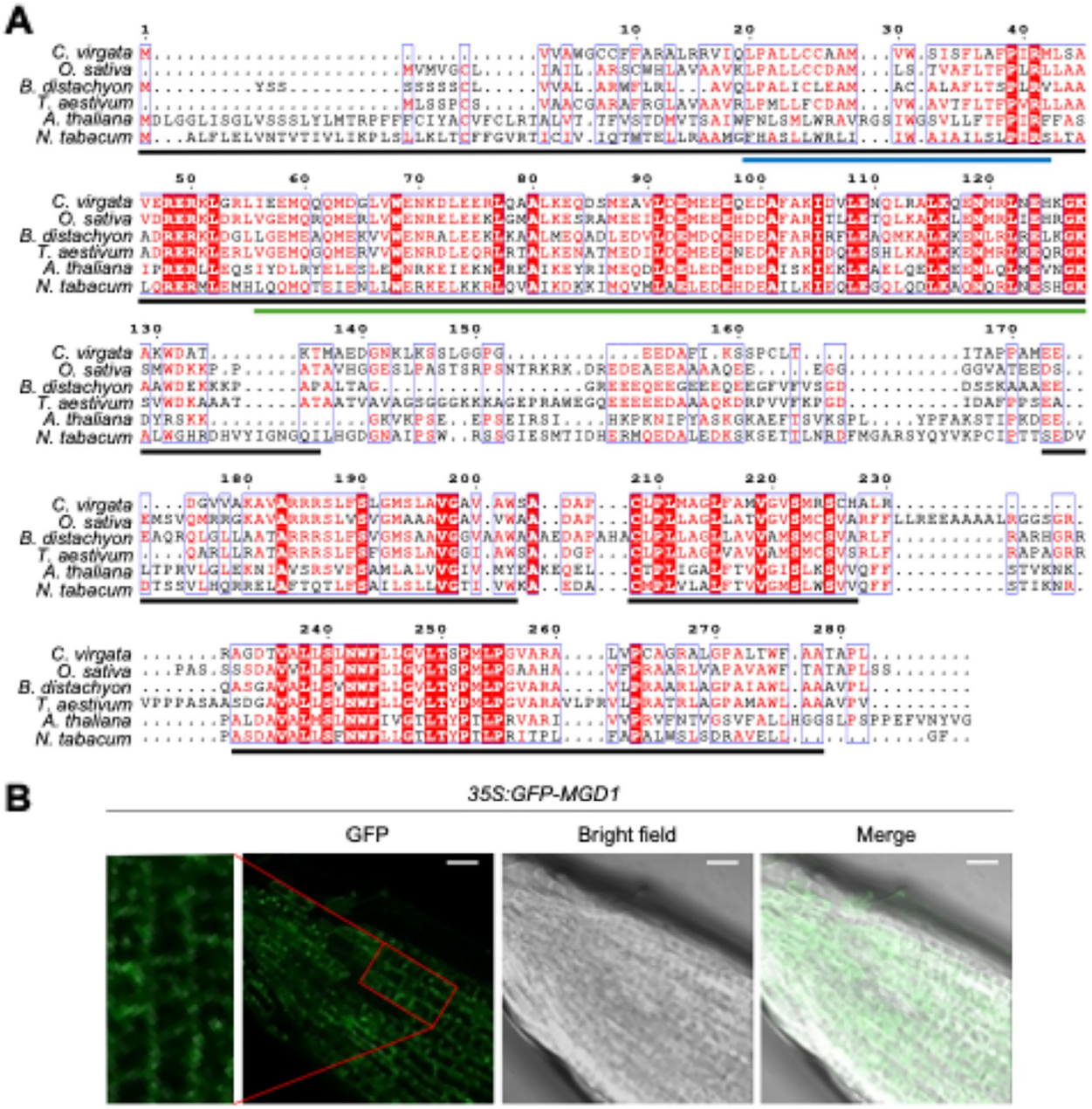

Fig. 6 Sequence conservation and subcellular localization of *MGD1*. **A** Amino acid sequence of *MGD1* and its homologues in other plant species. Accession numbers: *C. virgata* (ChlorisST30368), *O. sativa* (XP_015622376.1), *B. distachyon* (XP_003567507.1), *T. aestivum* (XP_044345791.1), *A. thaliana* (NP_001330291.1) and *N. tabacum* (XP_016510532.1). The highly conserved amino acids are indicated by a red background. The predicted α-helix regions are represented as black lines. The predicted transmembrane regions are represented as blue lines. The predicted coiled-coil region is represented as a green line. **B** Subcellular localization of *35S:GFP-MGD1* in the root cells of 4-day-old *Arabidopsis* plants. Scale bars = 20 μm.

was generated, and the fluorescence signal of *35S:GFP-MGD1* was observed. The GFP signal of *35S:GFP-MGD1* was observed as reticular and punctate signals within the cytoplasm, particularly around the nucleus, suggesting its localization to the Golgi apparatus (Fig. 6B).

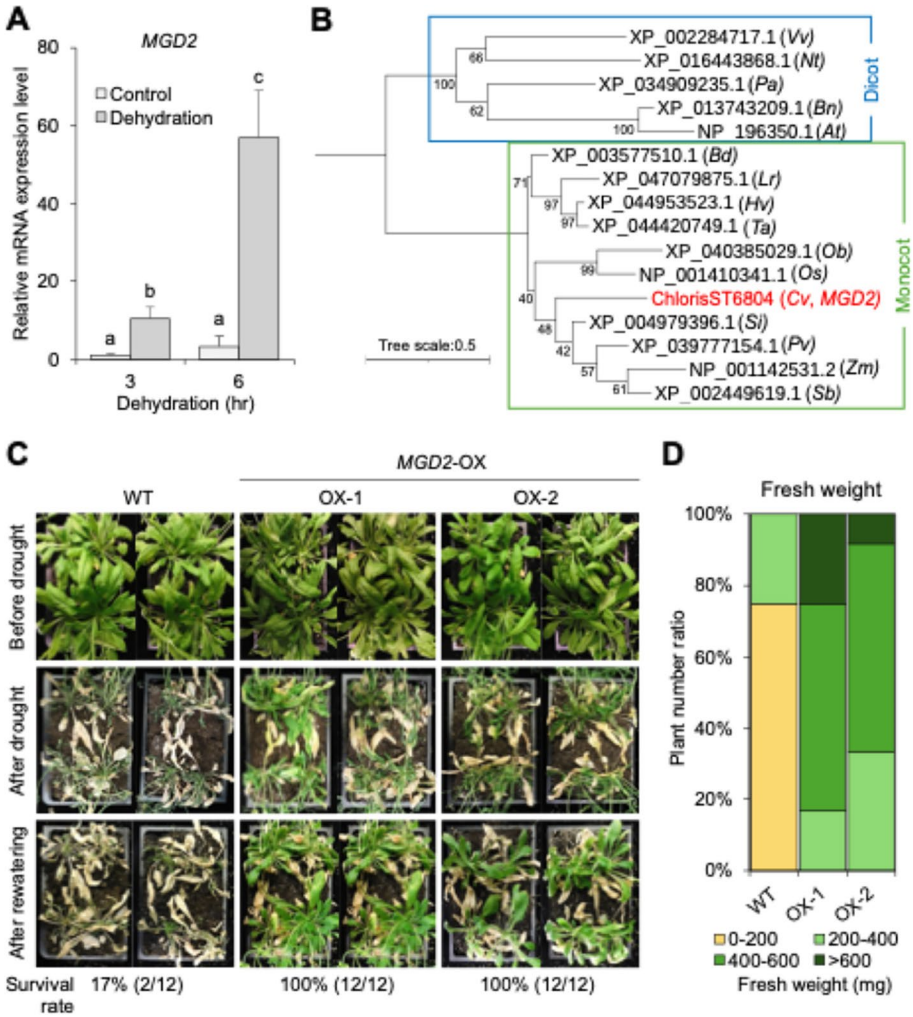

Fig. 7 *MGD2* promoted drought stress resistance in *Arabidopsis*. **A** Expression levels of the *MGD2* gene in *Chloris virgata* under dehydration stress. Seven-day-old plants were subjected to dehydration treatment or not for the indicated times. The error bars represent the means ± SDs from four replicated samples. The different letters above the bars indicate that the means are significantly different (One-way ANOVA with post-hoc Tukey HSD test ($P < 0.05$)). **B** Phylogenetic tree of MGD2 and related proteins in other species (*Vv, Vitis vinifera; Nt, Nicotiana tabacum; Pa, Populus alba; Bn, Brachypodium distachyon; At, Arabidopsis thaliana; Bd, Brachypodium distachyon; Lr, Lolium rigidum; Hv, Hordeum vulgare; Ta, Triticum aestivum; Ob, Oryza brachyantha; Os, Oryza sativa; Cv, Chloris virgata; Si, Setaria italica; Pv, Panicum virgatum; Zm, Zea mays; Sb, Sorghum bicolor*). The numbers at the branching sites indicate the posterior probability values for nodal support. **C**, **D** Survival rates (**C**) and fresh weights (**D**) of wild-type and *MGD2-OX Arabidopsis* plants under drought stress conditions. Four-week-old plants were subjected to drought treatment for 14 days and then rewatered for 2 days. Survival rates were calculated from the number of living plants after 2 days of rewatering (n=12). The fresh weights were measured after 2 days of rewatering (n=12)

MGD2-overexpressing *Arabidopsis* plants showed greater drought stress resistance than did WT plants

Compared with the control, the *ChlorisST6804* cDNA was more highly expressed after 3 hr of dehydration, with an approximately 10-fold change, and after 6 hr of dehydration, with a 56-fold change (Fig. 7A). Phylogenetic analysis revealed that the *ChlorisST6804* gene conserved in homologous genes from monocots and dicots, but the detailed functions of these homologous genes have not yet been reported (Fig. 7B).

After creating *Arabidopsis* plants overexpressing *ChlorisST6804* cDNA (OX-1 and OX-2) (Fig. S4D), the drought stress resistance of those plants that were grown on the soil for 4 weeks and withholding water for 2 weeks was analysed. Although only 17% of the wild-type plants survived, 100% of the *ChlorisST6804*-overexpressing plants survived and continued to grow after rewatering (Fig. 7C). The fresh weight of the *ChlorisST6804* cDNA-overexpressing plants was greater than those of the wild-type plants after rewatering (Fig. 7D). We named

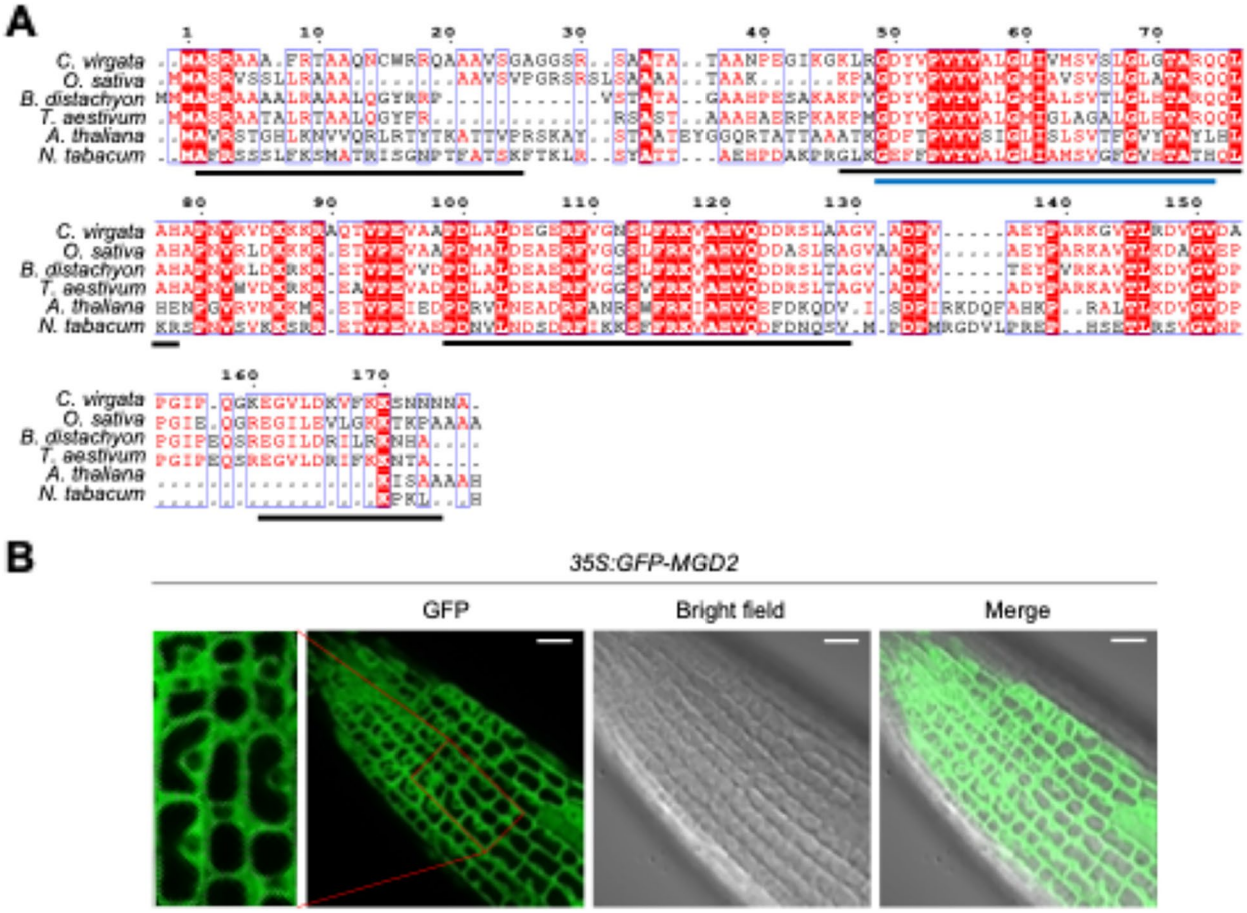

Fig. 8 Sequence conservation and subcellular localization of *MGD2*. **A** Amino acid sequence of *MGD2* and its homologues in other plant species. Accession numbers: *C. virgata* (ChlorisST6804), *O. sativa* (NP_001410341.1), *B. distachyon* (XP_003577510.1), *T. aestivum* (XP_044420749.1), *A. thaliana* (NP_196350.1) and *N. tabacum* (XP_016443868.1). The highly conserved amino acids are indicated by a red background. The predicted **α**-helix regions are represented as black lines. The predicted transmembrane region is represented as a blue line. **B** Subcellular localization of *35S:GFP-MGD2* in the root cells of 4-day-old *Arabidopsis* plants. Scale bars = 20 μm

the *ChlorisST6804* gene Mongolian Grassland plant Drought-stress resistance gene 2 (MGD2).

MGD2 encodes a functionally uncharacterized protein

The MGD2 protein contains 177 amino acids. To analyse the amino acid sequence similarity of MGD2 with other common plant species, sequence alignment analysis was performed (Fig. 8A). MGD2 showed high similarity to homologues from monocot species, such as *B. distachyon* (XP_003577510.1, 76.92%), *T. aestivum* (XP_044420749.1, 76.24%) and *O. sativa* (XP_001410341.1, 74.05%). The similarity with proteins from dicot species, such as *N. tabacum* (XP_016443868.1, 53.89%) and *Arabidopsis* (NP_196350.1, 49.75%), was lower than that with proteins from monocots, which is consistent with the results from the polygenetic tree that was constructed. These results indicate that the amino acid sequence of MGD2 shares a high identity with its monocot and dicot homologue proteins. A homologous gene in *Arabidopsis* (NP_196350.1, AT5G07330) has been described in several studies; for example, mutant lines of AT5G07330 presented increased sensitivity to $NaHCO_3$ [66], and its expression was upregulated in a zinc-finger protein (*ZAT12*)-overexpressing plant [67], and a putative heat-shock transcription factor A2 (*HsfA2*)-overexpressing plant [68]. However, the detailed characterizations of the molecular functions and the environmental stress responses remain poorly understood.

In the middle area of the MGD2 protein, extending approximately from amino acids 49–151, a highly identical conserved amino acid domain might exist. Nevertheless, the conserved domain has never been identified or reported in previous studies. First, we predicted the α-helix structure of the MGD2 protein on the AlphaFold3 server [35], which resulted in the identification

of four possible α-helix structures (Fig. S6B, Fig. 8A, represented as black lines). In addition, several transmembrane prediction servers, such as deepTMHMM [38], TOPCONS [39], and SOSUI [40], suggest that MGD2 might have one predicted transmembrane region (Fig. 8A, represented as a blue line). The predicted transmembrane regions corresponded to and overlapped with the α-helix structure, whose region was only predicted with high confidence (pDDT score over 70), and with the hydrophobic regions of MGD2 (Fig. S6A). Taken together, these predicted structural features suggest that MGD2 might be a membrane protein with one transmembrane helix.

To identify the subcellular localization of MGD2, transgenic *Arabidopsis* plants harbouring a GFP driven by the *CaMV35S* promoter were generated. The GFP signal of *35S:GFP-MGD2* was observed in the cytosol (Fig. 8B).

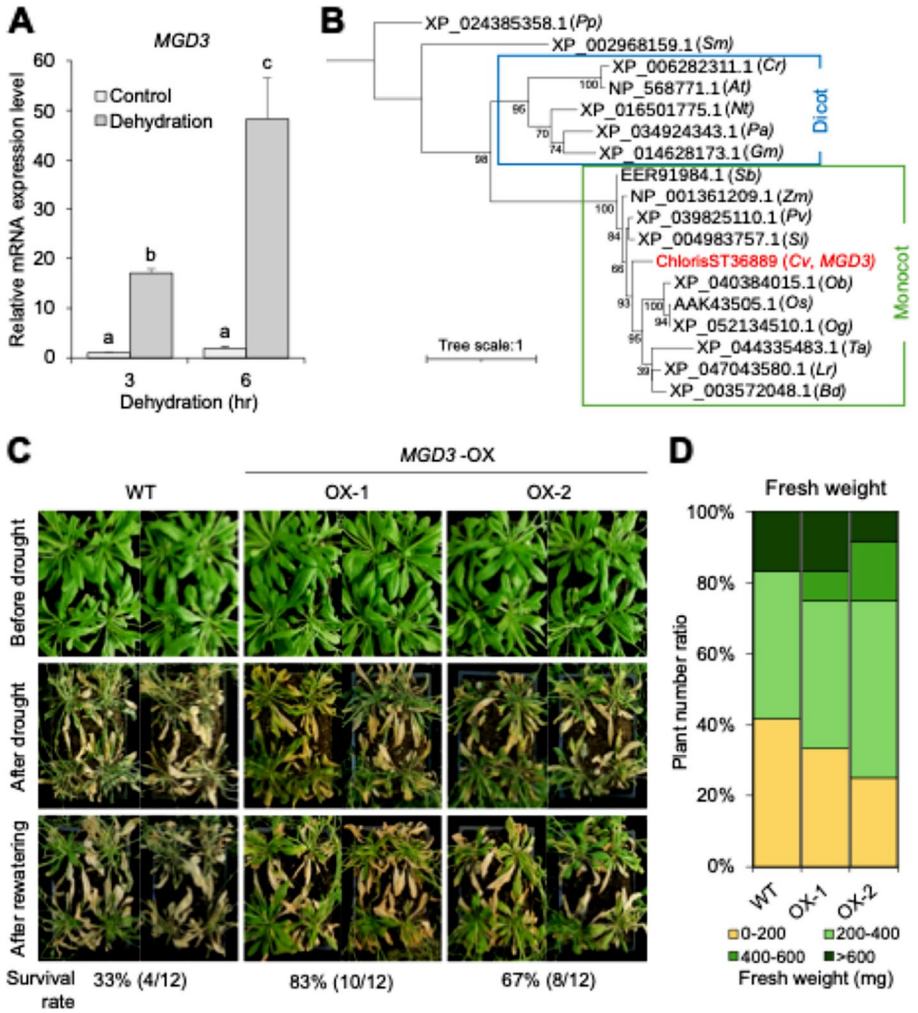

Fig. 9 *MGD3* promoted drought stress resistance in *Arabidopsis*. **A** Expression levels of the *MGD3* gene in *Chloris virgata* under dehydration stress. Seven-day-old plants were subjected to dehydration treatment or not for the indicated times. The error bars represent the means ± SDs from four replicated samples. The different letters above the bars indicate that the means are significantly different (One-way ANOVA with post-hoc Tukey HSD test ($P < 0.05$)). **B** Phylogenetic tree of MGD3 and related proteins in other species (*Pp, Physcomitrium patens; Sm, Selaginella moellendorffii; Cr, Capsella rubella; At, Arabidopsis thaliana; Nt, Nicotiana tabacum; Pa, Populus alba; Gm, Glycine max; Sb, Sorghum bicolor; Zm, Zea mays; Pv, Panicum virgatum; Si, Setaria italica; Cv, Chloris virgata; Ob, Oryza brachyantha; Os, Oryza sativa; Og, Oryza glaberrima; Ta, Triticum aestivum; Lr, Lolium rigidum; Bd, Brachypodium distachyon*). The numbers at the branching sites indicate the posterior probability values for nodal support. **C**, **D** Survival rates (**C**) and fresh weights (**D**) of wild-type and *MGD3-OX Arabidopsis* plants under drought stress conditions. Four-week-old plants were subjected to drought treatment for 14 days and then rewatered for 2 days. Survival rates were calculated from the number of living plants after 2 days of rewatering (n=12). The fresh weights were measured after 2 days of rewatering (n=12)

MGD3-overexpressing *Arabidopsis* plants showed greater drought stress resistance than did WT plants

The expression of *ChlorisST36889* cDNA was induced at an approximately 17-fold higher level by dehydration treatment for 3 hr and an approximately 48-fold higher level for 6 hr in comparison with control plants (Fig. 9A). *ChlorisST36889* was found to encode a novel gene that is conserved among homologous genes from various kinds of land plants; however, analyses of the detailed functions of the genes have not yet been reported (Fig. 9B).

When 4-week-old *ChlorisST36889* cDNA-overexpressing (OX-1 and OX-2) (Fig. S4E) plants were exposed to drought stress by withholding water from the plants for 2 weeks and continued rewatering for 2 days, the OX-1 and OX-2 overexpressing plants presented drought stress resistance, with survival rates of 83% and 67%, respectively, greater than those of wild-type *Arabidopsis*, whose survival rate was 33% (Fig. 9C). The fresh weight of the *MGD2*-overexpressing plants was relatively higher than those of the WT plants after rewatering (Fig. 9D). We named

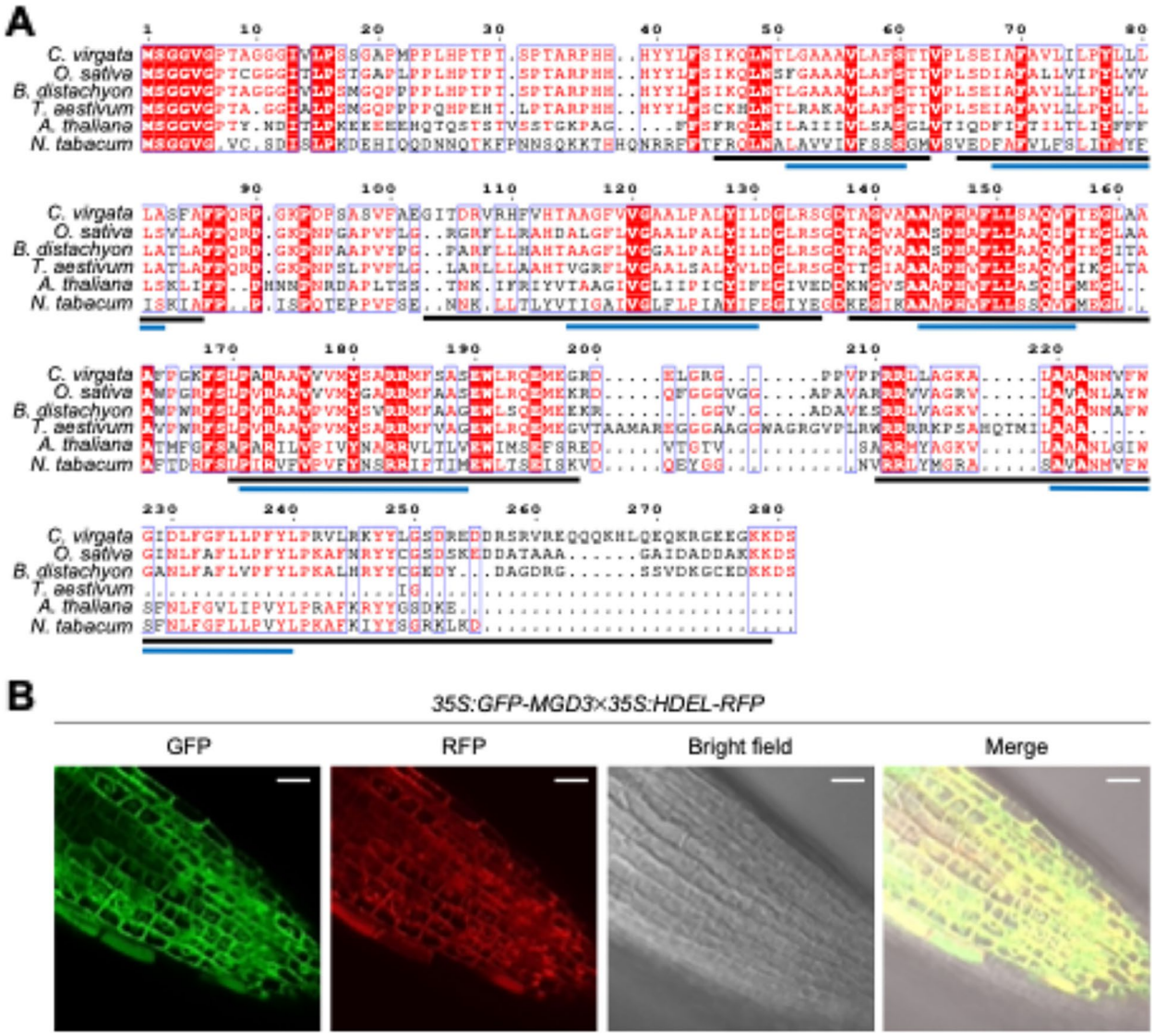

Fig. 10 Sequence conservation and subcellular localization of *MGD3*. **A** Amino acid sequence of *MGD3* and its homologues in other plant species. Accession numbers: *C. virgata* (ChlorisST36889), *O. sativa* (AAK43505.1), *B. distachyon* (XP_003572048.1), *T. aestivum* (XP_044335483.1), *A. thaliana* (NP_568771.1) and *N. tabacum* (XP_016501775.1). The highly conserved amino acids are indicated by a red background. The predicted α-helix regions are represented as black lines. The predicted transmembrane regions are represented as blue lines. **B** Subcellular localization of *35S:GFP-MGD3*×*35S:HDEL-RFP* in the root cells of 4-day-old *Arabidopsis* plants. Scale bars = 20 μm

the *ChlorisST36889* gene Mongolian Grassland plant Drought-stress resistance gene 3 (MGD3).

MGD3 encodes an uncharacterized and likely membrane-associated protein

MGD3 encodes a protein with 281 amino acids. By homology search analysis via BLAST, homologous proteins with similar amino acid lengths were identified from monocots and dicots (Fig. 10A). Amino acid sequence alignment revealed that the MGD3 protein shares high sequence similarity with its monocot homologues, i.e., 80% similarity with *O. sativa* (AAK43505.1), 79.4% similarity with *B. distachyon* (XP_003572048.1) and 58.6% similarity with *T. aestivum* (XP_044335483.1), but low sequence similarity with its dicot homologues, i.e., 52.3% similarity with *N. tabacum* (XP_016501775.1) and 52.2% similarity with *Arabidopsis* (NP_568771.1). These results indicate that the amino acid sequence of MGD3 shares a high identity with its monocot and dicot homologue proteins.

The middle region of the MGD3 protein, approximately from amino acids 120–195, contains a highly conserved amino acid domain, but the conserved domain has never been identified or reported before. The α-helix structure of the MGD3 protein was predicted by the AlphaFold3 server [35], resulting in the prediction of six antiparallel α-helix structures, with each α-helix being composed of more than 20 amino acids (Fig. S7B, Fig. 10A, represented as black lines). In addition, several transmembrane prediction servers, such as deepTMHMM [38] and TOPCONS [39], suggested that MGD3 might have 6 predicted transmembrane regions (Fig. 10A, represented as blue lines). The predicted transmembrane regions corresponded to and overlapped with the α-helix structure and hydrophobic regions of MGD3 (Fig. S7A). This predicted structural information suggested that MGD3 might be a membrane-associated protein with six putative transmembrane helices.

To analyse the possible function of the MGD3 protein at the cellular level, we observed the subcellular localization of the MGD3 protein. We generated transgenic *Arabidopsis* plants expressing the MGD3 protein fused to GFP driven by the *CaMV35S* promoter. Additionally, we crossed this *35S:GFP-MGD3* line with a *35S:HDEL-RFP* line, which carries an endoplasmic reticulum (ER) retention signal (HDEL) fused to RFP. An overlapping signal between GFP-MGD3 and HDEL-RFP was observed in the roots (Fig. 10B). These results suggested that MGD3 is localized to the ER or ER membrane.

Expression of stress-responsive genes in *MGD1*-, *MGD2*- and *MGD3*-overexpressing *Arabidopsis*

To explore the possible molecular functions of *MGD1*, *MGD2,* and *MGD3* in drought stress resistance-related signalling and ABA biosynthesis, the expression levels of drought stress-inducible genes in these overexpressing plants were analysed (Fig. 11). The expression levels of *dehydration responsive element binding factor 2A* (*DREB2A)*, *response to desiccation 29A (RD29A)* and *NCED3* in the transgenic (*MGD1*-OX-1, *MGD2*-OX-1, *MGD3*-OX-1, *CvNCED3*-OX-1, and *CvAREB1*-OX-1) and WT plants after dehydration treatments for 0, 15, 30 and 45 min, which were initiated by the transfer of these plants from ½ MS agar medium to parafilm, were subsequently analysed by qRT–PCR. Before drought treatment (0 min), no difference in the expression of the three stress-inducible genes was detected between any of the overexpressing plants and the WT plants. After drought treatment for 15–45 min, the expression of the drought stress-related transcription factor *DREB2A* was higher in the MGD1-OX plants than in the WT plants (Fig. 11A). The signalling factor *RD29A* and the ABA biosynthesis enzyme *NCED3* were also more highly induced in *MGD1*-OX plants than in the WT plants following drought treatments (Fig. 11A). In *MGD2*-OX plants, *NCED3* was strongly induced, and *RD29A* was slightly induced than in WT plants following drought treatments (Fig. 11B). In *MGD3*-OX plants, *RD29A* was slightly induced compared with that in the WT plants (Fig. 11C). These results suggest that these *MGD1*, *2* and *3* genes might strongly or partially activate drought stress resistance signalling, and the biosynthesis of the drought stress-resistant phytohormone ABA might be activated by *MGD2* and *MGD1*.

Discussion

In this study, we analysed the drought stress resistance of *C. virgata* (Fig. 1). Our previous research demonstrated that *C. virgata* has rapid germination and growth abilities in response to limited summer rainfall, with seeds initiating germination within 5 hr and showing rapid subsequent growth under the experimental conditions [21]. *C. virgata* has been reported to possess alkali resistance [69], but physiological studies on its resistance to other types of stress are limited. Seeds used in this study were collected from the desert steppe of Dornogobi Province, Mongolia, an area with an average annual precipitation of only 17.32 mm, significantly lower than the national average (150–400 mm) [70, 71]. These harsh environmental conditions likely selected *C. virgata*, which harbored genetic mutations that enabled adaptation to severe drought stress. Even under drought stress which rice and

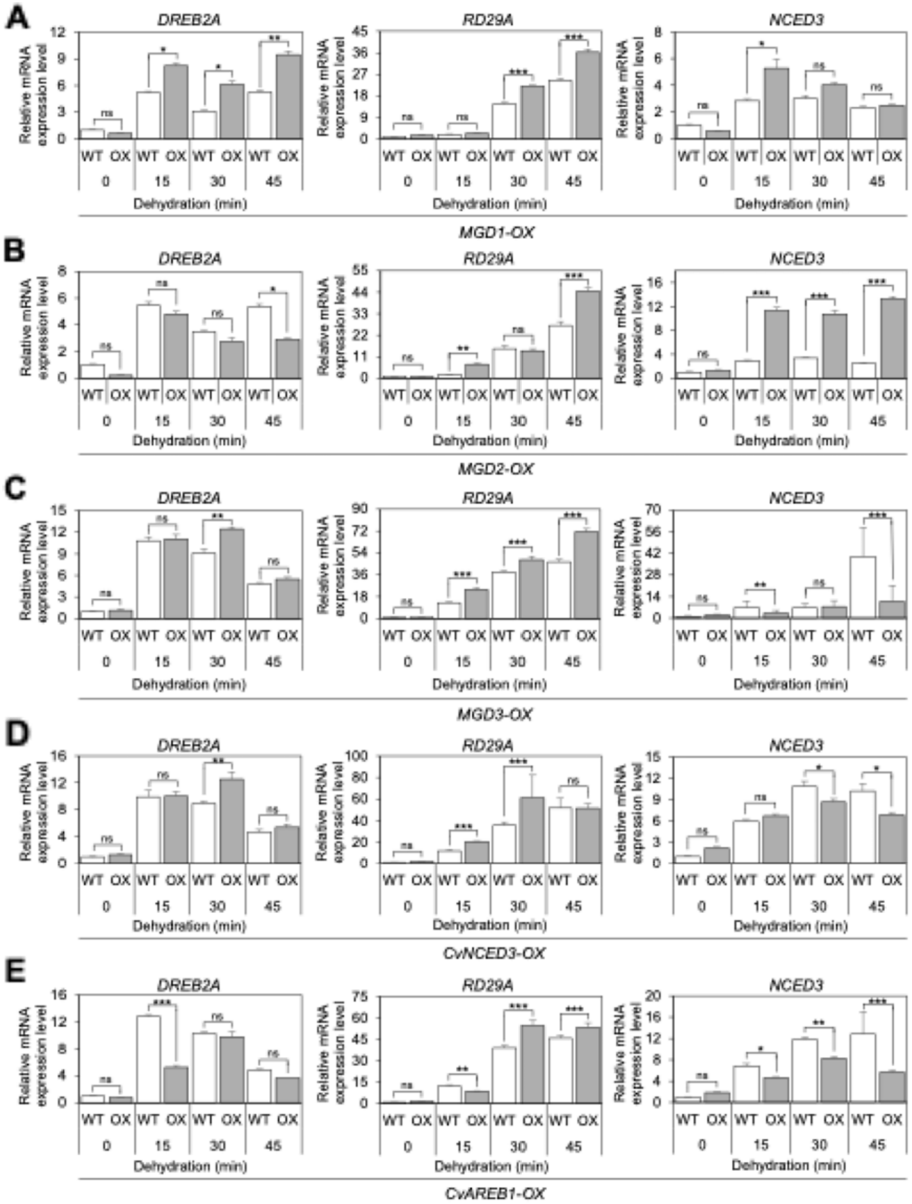

Fig. 11 Overexpression of the *MGD1*, *2,* and *3* genes partially promoted the expression of drought stress-inducible genes. **A**-**E** Expression analysis of stress-inducible genes in *MGD1*-OX (**A**), *MGD2*-OX (**B**), *MGD3*-OX (**C**), *CvNCED3*-OX (**D**), and *CvAREB1*-OX (**E**) transgenic plants and wild-type *Arabidopsis* under dehydration stress. Ten-day-old plants were treated with or without dehydration for the indicated times. The error bars represent the means ± SDs from four replicated samples. Statistical analyses were performed using Student's *t* test (ns = not significant; **P* < 0.05; ***P* < 0.01; ****P* < 0.001)

oat both decreased in chlorophyll content, *C. virgata* maintained high chlorophyll levels, indicating superior drought resistance (Figure 1).

Globally, approximately 50 species of the genus *Chloris* thrive in tropical regions, yet *C. virgata* is the only species found in Mongolia [72]. *C. virgata*, a member of the Poaceae family, has limited molecular characterization. In the field of weed science, a mutation in the 5-enolpyruvylshikimate-3-phosphare synthase (EPSPS) gene of *C. virgata* caused resistance to the glyphosate herbicide [73, 74]. Comparisons with other grass species such as the perennial *Leymus chinensis* (C3 grass) and the perennial *Hemarthria altissima* (C4 grass) suggest that *C. virgata* exhibits superior

carbon assimilation under moderate drought conditions [75, 76].

Among the grassland plants of Mongolia, several species exhibit high resistance to environmental stress, adapting to the harsh climatic conditions of the region. For example, *Caragana microphylla*, a dicot from the Fabaceae family, primarily grows in semiarid and desert areas of Northwest China and Mongolia. *C. microphylla* is known for its resistance to salt stress [77, 78]. Additionally, Agropyron cristatum L. (crested wheatgrass), belonging to the Poaceae family, is distributed across Eurasia, thriving in semiarid, arid steppe, and desert steppe regions. A. cristatum demonstrates excellent resistance to both cold and drought [79, 80]. When compared to these species, *C. virgata* exhibits particularly rapid germination, with coleoptiles emerging within 5 hr of germination treatment, as opposed to 1 day for A. cristatum and 3 days for C. microphylla [21]. Future analysis will reveal the similarities and differences among Chloris, Caragana, and Agropyron in terms of their ability to resist drought stress.

In this study, we performed the first *de novo* RNA-seq analysis of *C. virgata* under drought stress conditions, identifying 25,469 contigs with predicted ORFs (Fig. 3). This analysis provides new insights into the gene expression changes induced by dehydration, contributing to better understanding of drought resistance mechanisms. Previous studies identified 3,168 expressed sequence tags (ESTs) from alkali NaHCO3-treated *C. virgata* [81], and the complete chloroplast genome was sequenced [82]. Additionally, our earlier RNA-seq analysis of whole *C. virgata* organs during various developmental stages revealed 21,589 contigs [21]. However, this is the first large-scale transcriptome analysis focused on drought stress, offering a deeper insight into how *C. virgata* adapts to dry environments.

Comparative analyses within the genus *Chloris* suggest that drought resistance mechanisms may differ between species. For example, *Chloris gayana* exhibits resilience to sequential waterlogging and drought stress [83], and its salt-resistant phenotype is supported by salt-gland mechanisms [84, 85]. However, *C. virgata*, native to cold desert environments, may employ distinct physiological and molecular pathways for drought resistance. While a draft genome for *C. gayana* has been reported [86], transcriptomic studies of this species under stress conditions remain unexplored.

The results of our RNA-seq analysis revealed three gene expression clusters in *C. virgata*: genes highly expressed at both 3 hr and 6 hr of dehydration (Cluster 3), those expressed only at 3 hr (Cluster 1), and those expressed only at 6 hr (Cluster 2). Cluster 3 exhibited significant enrichment for ABA-related GO terms, including "cellular response to abscisic acid stimulus" and "abscisic acid-activated signaling pathway," similar to findings in drought-stressed *Arabidopsis* and rice [87, 88]. These results suggest that *C. virgata* employs an ABA-mediated mechanism to enhance drought resistance.

The molecular characterization of a known drought resistance-related ABA biosynthesis gene in *C. virgata* was conducted. Overexpression of *CvNCED3* in *Arabidopsis* enhanced drought resistance (Fig. 4A, B), consistent with previous reports on *NCED3* homologs in *Arabidopsis* and rice [5, 6]. The high amino acid similarity of *CvNCED3* to its rice (86%) and *Arabidopsis* (73%) counterparts, and the conservation of functional domains supports its role in ABA biosynthesis and drought resistance (Fig. S8). *AREB1* is a transcription factor essential for ABA signaling in drought resistance. In *Arabidopsis*, overexpression of the full-length *AREB1* does not enhance drought resistance, whereas a modified, active form (*AREB1ΔQT*) significantly improves drought resistance [50]. *OsAREB1* from rice has been shown to confer drought resistance when introduced into *Arabidopsis*, highlighting interspecies functional differences [60]. In this study, we introduced *CvAREB1* into *Arabidopsis* and evaluated its drought resistance. Overexpression of the full-length *CvAREB1* enhanced drought resistance compared to wild-type plants, resembling the function of *OsAREB1* (Fig. 4C, D). Sequence analysis revealed a high similarity between *CvAREB1* and *OsAREB1* (82%), while their similarity to *Arabidopsis AREB1* was lower (55%). The bZIP domain critical for transcriptional activity was highly conserved (Fig. S9). Interestingly, both *CvAREB1* and *OsAREB1* exhibit natural deletions in regions corresponding to parts of *Arabidopsis AREB1*, which may contribute to their enhanced drought resistance. These findings suggest that *CvAREB1* functions through mechanisms similar to *OsAREB1* to improve drought stress resistance.

To identify novel drought-resistance genes, we isolated the 60 drought-inducible *C. virgata* genes and characterized ten poorly studied candidates through overexpression in *Arabidopsis*. Among these, *MGD1* conferred significant drought resistance, with transgenic plants showing higher fresh weight after rewatering (Fig. 5). Enhanced expression of drought-responsive genes such as *RD29A*, *DREB2A*, and *NCED3* in *MGD1*-overexpressing plants suggests a role for *MGD1* in both ABA-dependent and independent pathways (Fig. 11A). Structural predictions and GFP-tagged localization studies suggest that *MGD1* is a Golgi-associated transmembrane protein (Fig. 6B). Transmembrane proteins, including aquaporins and ER-membrane-associated E3 ubiquitin ligases, have been reported as their roles in stress response [89–93]. The overexpression of *Arabidopsis NHX5*, the sodium/

hydrogen transporter localizes to the Golgi, improves drought resistance in *Broussonetia papyrifera* [94]. As these reports suggested that plant membrane proteins contribute to increased drought stress resistance, a detailed prediction and analysis of MGD1 localization would be interesting. The N-terminal conserved region of MGD1 protein participates in intermolecular interactions by forming a coiled-coil superhelix (Fig. 6A, Fig. S5). Several proteins are predicted to form a coiled-coil attachment to Golgi membranes at the C-terminal transmembrane helix. Golgins have a long coiled coil consisting of at least 500 residues and extend 100–400 nm [95]. They form part of the Golgi matrix and play a role in vesicle tethering [96, 97]; however, the mechanisms by which these proteins control Golgi organization remain largely unknown. In *Arabidopsis,* six putative golgins have been isolated, and two of these proteins possess C-terminal transmembrane domains and share similarities with the mammalian protein *golgin-84*, whereas two others (one of which is *GDAP1*) are characterized by C-terminal GRAB domains. The remaining two proteins share regions of significant similarity with the mammalian golgins *TMF* and *p115* [98]. Among the other Golgi membrane-anchored coiled-coil proteins, the most obvious are *SNARE* proteins, which form four helical bundles of coiled coils to drive the membrane fusion of vesicles [95]. Several *SNARE* proteins are located on the Golgi apparatus membrane and are evolutionarily conserved from yeast to animals and plants. The *SNAP33* gene, a protein belonging to the *SNARE* superfamily initially identified in mammalian neurons, is localized to the plasma membrane and is expressed ubiquitously in all tissues of *Arabidopsis*. Although *SNAP33* is not typically associated with the Golgi apparatus, the expression of *GsSNAP33* in wild soybean (*Glycine soja*) is induced by salt, alkali, ABA, and drought. Furthermore, the overexpression of the *GsSNAP33* gene in *Arabidopsis* improved drought stress resistance; increased germination rates, root lengths, and photosynthesis activity, and upregulated the expression levels of various stress-responsive marker genes in overexpressing plants compared with those in wild-type plants [99]. Compared with those of other Golgin proteins, the full-length amino acid sequence of *MGD1* is relatively short and does not exhibit amino acid homology with other *SNARE* proteins, which might indicate that *MGD1* is distinct from other known Golgin proteins. *MGD1* has been shown to increase drought stress resistance in *Arabidopsis*, suggesting that its significant role is associated with the Golgi apparatus during drought stress conditions.

The gene *MGD2*, induced by dehydration stress, enhances drought resistance (Fig. 7). Homologous proteins for MGD2 are unknown, with no identifiable domains or motifs. *MGD2*-overexpressing plants showed increased *NCED3* mRNA levels compared to WT (Fig. 11B), suggesting its role in ABA-dependent drought resistance. Structural predictions indicate four α-helices in MGD2, with the second α-helix potentially being transmembrane (Fig. 8A, Fig. S6). While InterPro and SOSUI predict a cytoplasmic N-terminus, TOPCONS suggests an extracellular one, leaving its topology uncertain. *35S:GFP-MGD2* transgenic plants indicate that MGD2 was localized to the cytoplasm (Fig. 8B), contradicting transmembrane predictions, necessitating further validation.

The MGD3 gene conferred higher drought resistance than WT when overexpressed in *Arabidopsis* (Fig. 9). Expression levels of *RD29A* and *DREB2A* increased slightly in *MGD3*-overexpressing plants, while *NCED3* expression remained unchanged, suggesting ABA-independent drought resistance (Fig. 11C). MGD3 lacks known functional domains but has homologous proteins in various plant species, though their functions remain unreported. Predictions indicate six α-helix regions in MGD3, overlapping with hydrophobic amino acids and likely forming a multipass transmembrane protein, such as a channel or transporter protein [89] (Fig. 10A, Fig. S7). GFP-MGD3 protein localized to the ER (Fig. 10B). Given the characteristic localization of the MGD3 protein in cells and the increased drought stress resistance caused by MGD3 in plants, unknown but valuable functions of the MGD3 protein should be revealed in the future.

Conclusion

In conclusion, this study revealed that Mongolian grassland plant *C. virgata* is highly resistant to drought stress. By *de novo* RNA-seq-based transcriptome analysis, 25,469 protein-coding transcripts were determined, and 1,219 cDNAs were identified as drought stress-inducible genes from *C. virgata* exposed to drought stress for 3 hr and 6 hr. After the transformation of approximately ten drought-inducible genes into *Arabidopsis* and the exposure of these transformants to drought stress, the gene that presented the strongest drought-stress resistance was named *MGD1*. The MGD1 protein is conserved from monocots to dicots, has not been previously reported, and is predicted to possess one transmembrane domain and one coiled-coil domain. *MGD2*- and *MGD3*-overexpressing *Arabidopsis* plants also presented higher drought stress resistance than did wild-type plants. The MGD2 and MGD3 proteins are not well characterized but are predicted to possess putative transmembrane domains. The drought stress resistance promoted by the *MGD1*, *2,* and *3* genes suggests that these genes may contribute to molecular breeding in agriculture and the

improvement of the dilapidating desert area of Mongolia. These searches for functional genes from unutilized wild plants could be effective in identifying unknown but valuable genes in the future.

Supplementary Information

The online version contains supplementary material available at https://doi.org/10.1186/s12870-025-06046-3.

Supplementary Material 1. Table S1. Sequences of the primers used in this study. Table S2. Summary of raw and clean read statistics from *Chloris virgata* after Illumina sequencing. Table S3. The top 60 most significantly upregulated genes in *Chloris virgata* after 3 hr of dehydration. The *MGD1*, *MGD2,* and *MGD3* genes are highlighted in bold letters and underlined with three asterisks, and the selected genes as preliminary *MGD* candidate genes that transformed to *Arabidopsis* are highlighted in bold letters with one asterisk. Table S4. The top 60 most significantly upregulated genes in *Chloris virgata* after 6 hr of dehydration. The *MGD1*, *MGD2,* and *MGD3* genes are highlighted in bold letters and underlined with three asterisks, and the selected genes as preliminary *MGD* candidate genes that transformed to *Arabidopsis* are highlighted in bold letters with one asterisk. Table S5. The top 60 most significantly downregulated genes in *Chloris virgata* after 3 hr of dehydration. Table S6. The top 60 most significantly downregulated genes in *Chloris virgata* after 6 hr of dehydration. Fig. S1. Osmotic stress sensitivity of *Chloris virgata*. (A, B) Plant fresh weight (A) and shoot length (B) of *Chloris virgata*, rice, and oat under mannitol treatment. Seven-day-old seedlings grown on ½ MS medium were transplanted to ½ MS medium supplemented with or without various concentrations of mannitol. The fresh weight and shoot length were measured after 3 weeks of treatment with mannitol. The three highest values were converted to 100% in each treatment.n=18. Fig. S2. PCA of gene expression profiles based on transcripts per million (TPM) counts (log10-transformed). The plot shows the distribution of plant samples along the first two components, PC1 (38.32% variance explained) and PC2 (8.04% variance explained). The treatment series includes control samples at 3 hr and 6 hr, and drought samples at 3 hr and 6 hr. Fig. S3. Gene Ontology (GO) analysis of downregulated genes in *Chloris virgata*. (A) Venn diagram showing the downregulated genes (p<0.05, fold change<-1.5) in *Chloris virgata* after dehydration for 3 hr and 6 hr. (B) Enrichment of GO annotations in biological process categories for genes downregulated after treatment with both 3 hr and 6 hr of dehydration. The y-axis indicates the pathway name, and the x-axis indicates the gene ratio. The p-adjusted value is represented by the colour of each dot, and the number of DEGs is represented by the size of each dot. Fig. S4. Expression analysis of transgenes in transgenic *Arabidopsis* overexpression lines. (A-E) Transgene expression levels in *CvNCED3-OX* (A), *CvAREB1-OX* (B), *MGD1-OX* (C), *MGD2-OX,* (D), and *MGD3-OX* (E) compared with those in WT. The error bars represent the means ± SDs from four replicated samples. The different letters above the bars indicate that the means are significantly different (One-way ANOVA with post-hoc Tukey HSD test (P< 0.05)). Fig. S5. Structure prediction of MGD1. (A)Hydropathy plot of MGD1. The plot was generated using the NovoPro server [35] with the Kyte & Doolittle scale [42]. (B, C) The structural models and predicted alignment errors of the MGD1 monomer (B) and dimer (C), were generatedusing the AlphaFold3 server [43]. The N- and C-termini are indicated by the letters N and C, respectively. Fig. S6. Structure prediction of MGD2. (A) Hydropathy plot of MGD2. The plot was generated using the NovoPro server with the Kyte & Doolittle scale. (B) The structural models and predicted alignment errors of MGD2 were generatedusing the AlphaFold3 server. The N- and C-termini are indicated by the letters N and C, respectively. Fig. S7. Structure prediction of MGD3. (A) Hydropathy plot of MGD3. The plot was generated using the NovoPro server with the Kyte & Doolittle scale. (B) The structural models and predicted alignment errors of MGD3 were generatedusing the AlphaFold3 server. The N- and C-termini are indicated by the letters N and C, respectively. Fig. S8. Amino acid sequence alignment of *CvNCED3* (ChlorisST40659) with *AtNCED3* (accession AEE75526.1), and *OsNCED3* (accession NP_001405315.1). Identical amino acids are indicated in black and grey. The red line represents the RPE65 domain. The green line indicates possible AC motifs. Fig. S9. Amino acid sequence alignment of *CvAREB1* (ChlorisST30712) with *AtAREB1* (accession BAB12404.1), and *OsAREB1* (accession NP_001403850.1). Identical amino acids are indicated in black and grey. The red line represents the bZIP domain. The yellow highlighted regions indicate the deleted sequence of the *AtAREB1*△*QT* constitutively active form.

Acknowledgment
We would like to thank T. Nakagawa, Shimane University, for providing the pGWB cloning vectors. We would like to thank M. Tominaga, Waseda University, for providing the 35Spro:HDEL-RFP seeds.

Authors' contributions
T.N., A.Y., G.N., J.B., B.D. and T.A. conceived and designed the experiments. G.N., B.Bu., B.Bo., S.K., H.O., T.M, and A.Y. performed the experiments and phylogenetic and molecular biology analyses. K.M., A.K., M.S. and A.M. performed the sequencing and de novo transcriptome analyses. G.N., A.Y., K.M., T.M. and T.N. contributed to manuscript preparation.

Funding
This work was supported in part by grants from the Science and Technology Research Partnership for Sustainable Development (SATREPS), the Japan Science and Technology Agency (JST)/Japan International Cooperation Agency (JICA) [grant number: JPMJSA1906] to T.N. B.D. J.B. and T.A., the NARO Bio-oriented Technology Research Advancement Institution (BRAIN) to T.N. and T.A., CREST, the Japan Science and Technology Agency to T.N. and T.A., and grants from JSPS KAKENHI (grant numbers: JP18H02140 and 24H00502) to T.N. This work was partially supported by Cabinet Office, Government of Japan, Moonshot R&D Program for Agriculture, Forestry and Fisheries (funding agency: Bio-oriented Technology Research Advancement Institution, No. JPJ009237) to K.M.

Data availability
The sequenced raw reads generated during the current study have been submitted to DNA Data Bank of Japan Sequence Read Archive (DDJB SRA) under the accession number PRJDB18577. Other relevant data analysed during this study are included in this published article and its additional information files.

Declarations

Ethics approval and consent to participate
C. virgata seeds were harvested from the native grassland of Dornogovi Province, Mongolia. The voucher specimens were deposited in the Plant Herbarium Library of the Laboratory of Plant Biotechnology, National University of Mongolia (voucher number: 17.29.01) and identified by Dr. Shagdar Dariimaa. Experimental research on plants, including seed collection and transfer, was conducted with approval from the Ministry of Environment and Climate Change of Mongolia, in full compliance with all relevant institutional and national regulations and legislation.

Consent for publication
Not applicable.

Competing interests
The authors declare no competing interests.

Author details
[1]Laboratory of Plant Chemical Biology, Graduate School of Biostudies, Kyoto University, Sakyo-ku, Kyoto 606-8502, Japan. [2]RIKEN Center for Sustainable Resource Science, Tsurumi-ku, Yokohama, Kanagawa 230-0045, Japan. [3]Kihara Institute for Biological Research, Yokohama City University, Totsuka-ku, Yokohama, Kanagawa 244-0813, Japan. [4]Baton Zone Program, RIKEN, Tsurumi-ku, Yokohama, Kanagawa 230-0045, Japan. [5]School of Information and Data Sciences, Nagasaki University, Bunkyo-machi, Nagasaki 852-8521, Japan. [6]School of Engineering and Technology, National University of Mongolia, Ulaanbaatar 14201, Mongolia. [7]Graduate School of Agricultural and Life Sciences, The University of Tokyo, Bunkyo-ku, Tokyo 113-8657, Japan.

Received: 1 August 2024 Accepted: 1 January 2025
Published online: 11 January 2025

References

1. The Ministry of the Environment of Japan CCAO Policy Planning Division, Global Environment Bureau. Global Climate Model Calculation Results. 2013. Climate change in Mongolia (dataset ID: GCM60_ADAPT2013). Available from: https://www.env.go.jp/content/900448010.pdf
2. Harb A, Krishnan A, Ambavaram MMR, Pereira A. Molecular and physiological analysis of drought stress in arabidopsis reveals early responses leading to acclimation in plant growth. Plant Physiol. 2010;154(3):1254–71.
3. Hu C, Elias E, Nawrocki WJ, Croce R. Drought affects both photosystems in *Arabidopsis thaliana*. New Phytol. 2023;240(2):663–75.
4. Farooq M, Basra SMA, Wahid A, Ahmad N, Saleem BA. Improving the drought tolerance in rice (Oryza sativa L.) by exogenous application of salicylic acid. J Agron Crop Sci. 2009;195(4):237–46.
5. Iuchi S, Kobayashi M, Taji T, Naramoto M, Seki M, Kato T, et al. Regulation of drought tolerance by gene manipulation of 9- *cis* -epoxycarotenoid dioxygenase, a key enzyme in abscisic acid biosynthesis in *Arabidopsis*. Plant J. 2001;27(4):325–33.
6. Hwang SG, Chen HC, Huang WY, Chu YC, Shii CT, Cheng WH. Ectopic expression of rice OsNCED3 in Arabidopsis increases ABA level and alters leaf morphology. Plant Sci. 2010;178(1):12–22.
7. Huang Y, Guo Y, Liu Y, Zhang F, Wang Z, Wang H, et al. 9-cis-Epoxycarotenoid Dioxygenase 3 regulates plant growth and enhances multi-abiotic stress tolerance in rice. Front Plant Sci. 2018;9:162.
8. Sakuma Y, Maruyama K, Osakabe Y, Qin F, Seki M, Shinozaki K, et al. Functional analysis of an *arabidopsis* transcription factor, DREB2A, involved in drought-responsive gene expression. Plant Cell. 2006;18(5):1292–309.
9. Mizoi J, Kanazawa N, Kidokoro S, Takahashi F, Qin F, Morimoto K, et al. Heat-induced inhibition of phosphorylation of the stress-protective transcription factor DREB2A promotes thermotolerance of Arabidopsis thaliana. J Biol Chem. 2019;294(3):902–17.
10. Mallikarjuna G, Mallikarjuna K, Reddy MK, Kaul T. Expression of OsDREB2A transcription factor confers enhanced dehydration and salt stress tolerance in rice (Oryza sativa L.). Biotechnol Lett. 2011;33(8):1689–97.
11. Yamaguchi-Shinozaki K, Koizumi M, Urao S, Shinozaki K. Molecular cloning and characterization of 9 cDNAs for genes that are responsive to desiccation in arabidopsis thaliana: Sequence analysis of one cDNA clone that encodes a putative transmembrane channel protein. Plant Cell Physiol. 1992;33(3):217–24.
12. Yamaguchi-Shinozaki K, Shinozaki K. Arabidopsis DNA encoding two desiccation-responsive rd29 genes. Plant Physiol. 1993;101(3):1119–20.
13. Seki M, Narusaka M, Ishida J, Nanjo T, Fujita M, Oono Y, et al. Monitoring the expression profiles of 7000 *Arabidopsis* genes under drought, cold and high-salinity stresses using a full-length cDNA microarray. Plant J. 2002;31(3):279–92.
14. Ghorbani R, Alemzadeh A, Razi H. Microarray analysis of transcriptional responses to salt and drought stress in Arabidopsis thaliana. Heliyon. 2019;5(11):e02614.
15. Sakamoto H, Maruyama K, Sakuma Y, Meshi T, Iwabuchi M, Shinozaki K, et al. Arabidopsis Cys2/His2-type zinc-finger proteins function as transcription repressors under drought, cold, and high-salinity stress conditions. Plant Physiol. 2004;136(1):2734–46.
16. Qin L, He H, Yang L, Zhang H, Li J, Zhu Y, et al. AtZAT10/STZ1 improves drought tolerance and increases fiber yield in cotton. Front Plant Sci. 2024;15:1464828.
17. Sirohi P, Yadav BS, Afzal S, Mani A, Singh NK. Identification of drought stress-responsive genes in rice (Oryza sativa) by meta-analysis of microarray data. J Genet. 2020;99(1):35.
18. Koops P, Pelser S, Ignatz M, Klose C, Marrocco-Selden K, Kretsch T. EDL3 is an F-box protein involved in the regulation of abscisic acid signalling in Arabidopsis thaliana. J Exp Bot. 2011;62(15):5547–60.
19. Li H, Yao W, Fu Y, Li S, Guo Q. De novo assembly and discovery of genes that are involved in drought tolerance in Tibetan Sophora moorcroftiana. PloS One. 2015;10:1 e111054.
20. Li S, Fan C, Li Y, Zhang J, Sun J, Chen Y, et al. Effects of drought and salt-stresses on gene expression in Caragana korshinskii seedlings revealed by RNA-seq. BMC Genomics. 2016;17(1):200.
21. Bolortuya B, Kawabata S, Yamagami A, Davaapurev BO, Takahashi F, Inoue K, et al. Transcriptome analysis of Chloris virgata, which shows the fastest germination and growth in the major Mongolian Grassland plant. Front Plant Sci. 2021;12:684987.
22. Stoop J, Williamson J, Masonpharr D. Mannitol metabolism in plants: a method for coping with stress. Trends Plant Sci. 1996;1(5):139–44.
23. Yamaguchi-Shinozaki K, Shinozaki K. A novel cis-acting element in an Arabidopsis gene is involved in responsiveness to drought, low-temperature, or high-salt stress. Plant Cell. 1994;6(2):251–64.
24. Porra RJ, Thompson WA, Kriedemann PE. Determination of accurate extinction coefficients and simultaneous equations for assaying chlorophylls a and b extracted with four different solvents: verification of the concentration of chlorophyll standards by atomic absorption spectroscopy. Biochim Biophys Acta BBA - Bioenerg. 1989;975(3):384–94.
25. Qin F, Sakuma Y, Tran LSP, Maruyama K, Kidokoro S, Fujita Y, et al. *Arabidopsis* DREB2A-interacting proteins function as RING E3 ligases and negatively regulate plant drought stress-responsive gene expression. Plant Cell. 2008;20(6):1693–707.
26. R Foundation for Statistical Computing, Vienna. R Core Team (2022) R: A Language and Environment for Statistical Computing. Available from: https://www.R-project.org
27. Nakagawa T, Kurose T, Hino T, Tanaka K, Kawamukai M, Niwa Y, et al. Development of series of gateway binary vectors, pGWBs, for realizing efficient construction of fusion genes for plant transformation. J Biosci Bioeng. 2007;104(1):34–41.
28. Nakagawa T, Suzuki T, Murata S, Nakamura S, Hino T, Maeo K, et al. Improved gateway binary vectors: high-performance vectors for creation of fusion constructs in transgenic analysis of plants. Biosci Biotechnol Biochem. 2007;71(8):2095–100.
29. Clough SJ, Bent AF. Floral dip: a simplified method for *Agrobacterium*-mediated transformation of *Arabidopsis thaliana*. Plant J. 1998;16(6):735–43.
30. Montgomery SA, Tanizawa Y, Galik B, Wang N, Ito T, Mochizuki T, et al. Chromatin organization in early land plants reveals an ancestral association between H3K27me3, transposons, and constitutive heterochromatin. Curr Biol. 2020;30(4):573-588.e7.
31. Katoh K, Rozewicki J, Yamada KD. MAFFT online service: multiple sequence alignment, interactive sequence choice and visualization. Brief Bioinform. 2019;20(4):1160–6.
32. Trifinopoulos J, Nguyen LT, von Haeseler A, Minh BQ. W-IQ-TREE: a fast online phylogenetic tool for maximum likelihood analysis. Nucleic Acids Res. 2016;44(W1):W232-5.
33. Letunic I, Bork P. Interactive Tree Of Life (iTOL) v5: an online tool for phylogenetic tree display and annotation. Nucleic Acids Res. 2021;49(W1):W293-6.
34. Robert X, Gouet P. Deciphering key features in protein structures with the new ENDscript server. Nucleic Acids Res. 2014;42(W1):W320-4.
35. Abramson J, Adler J, Dunger J, Evans R, Green T, Pritzel A, et al. Accurate structure prediction of biomolecular interactions with AlphaFold 3. Nature. 2024;630(8016):493–500.
36. Slabinski L, Jaroszewski L, Rychlewski L, Wilson IA, Lesley SA, Godzik A. XtalPred: a web server for prediction of protein crystallizability. Bioinformatics. 2007;23(24):3403–5.
37. Paysan-Lafosse T, Blum M, Chuguransky S, Grego T, Pinto BL, Salazar GA, et al. InterPro in 2022. Nucleic Acids Res. 2023;51(D1):D418-27.
38. Hallgren J, Tsirigos KD, Pedersen MD, Almagro Armenteros JJ, Marcatili P, Nielsen H, et al. DeepTMHMM predicts alpha and beta transmembrane proteins using deep neural networks. Bioinformatics. 2022;38(14):3759–66.
39. Tsirigos KD, Peters C, Shu N, Käll L, Elofsson A. The TOPCONS web server for consensus prediction of membrane protein topology and signal peptides. Nucleic Acids Res. 2015;43(W1):W401-7.
40. Hirokawa T, Boon-Chieng S, Mitaku S. SOSUI: classification and secondary structure prediction system for membrane proteins. Bioinformatics. 1998;14(4):378–9.
41. Mariani V, Biasini M, Barbato A, Schwede T. lDDT: a local superposition-free score for comparing protein structures and models using distance difference tests. Bioinformatics. 2013;29(21):2722–8.

42. Novopro Labs. Available from: https://www.novoprolabs.com/tools/protein-hydropathy
43. Kyte J, Doolittle RF. A simple method for displaying the hydropathic character of a protein. J Mol Biol. 1982;157(1):105–32.
44. Możdżeń K, Bojarski B, Rut G, Migdałek G, Repka P, Rzepka A. Effect of drought stress induced by mannitol on physiological parameters of maize (Zea Mays L.) seedlings and plants. J Microbiol Biotechnol Food Sci. 2015;4(special issue 2(Biotechnology)):86–91.
45. Behnam B, Iuchi S, Fujita M, Fujita Y, Takasaki H, Osakabe Y, et al. Characterization of the promoter region of an Arabidopsis gene for 9-cis-Epoxycarotenoid Dioxygenase involved in dehydration-inducible transcription. DNA Res. 2013;20(4):315–24.
46. Kalladan R, Lasky JR, Sharma S, Kumar MN, Juenger TE, Des Marais DL, et al. Natural variation in 9-Cis-Epoxycartenoid Dioxygenase 3 and ABA accumulation. Plant Physiol. 2019;179(4):1620–31.
47. Molinari MDC, Fuganti-Pagliarini R, Marin SRR, Ferreira LC, Barbosa DDA, Marcolino-Gomes J, et al. Overexpression of AtNCED3 gene improved drought tolerance in soybean in greenhouse and field conditions. Genet Mol Biol. 2020;43(3):e20190292.
48. Collin A, Daszkowska-Golec A, Szarejko I. Updates on the Role of Abscisic acid insensitive 5 (ABI5) and Abscisic acid-responsive element binding factors (ABFs) in ABA signaling in different developmental stages in plants. Cells. 2021;10(8):1996.
49. Yoshida T, Mogami J, Yamaguchi-Shinozaki K. ABA-dependent and ABA-independent signaling in response to osmotic stress in plants. Curr Opin Plant Biol. 2014;21:133–9.
50. Fujita Y, Fujita M, Satoh R, Maruyama K, Parvez MM, Seki M, et al. AREB1 is a transcription activator of novel ABRE-dependent ABA signaling that enhances drought stress tolerance in *Arabidopsis*. Plant Cell. 2005;17(12):3470–88.
51. Oh SJ, Song SI, Kim YS, Jang HJ, Kim SY, Kim M, et al. Arabidopsis CBF3/DREB1A and ABF3 in transgenic rice increased tolerance to abiotic stress without stunting growth. Plant Physiol. 2005;138(1):341–51.
52. Fuganti-Pagliarini R, Ferreira LC, Rodrigues FA, Molinari HBC, Marin SRR, Molinari MDC, et al. Characterization of soybean genetically modified for drought tolerance in field conditions. Front Plant Sci. 2017;8:448.
53. Grabherr MG, Haas BJ, Yassour M, Levin JZ, Thompson DA, Amit I, et al. Full-length transcriptome assembly from RNA-Seq data without a reference genome. Nat Biotechnol. 2011;29(7):644–52.
54. Huang X, Wang J, Aluru S, Yang SP, Hillier L. PCAP: a whole-genome assembly program. Genome Res. 2003;13(9):2164–70.
55. Fu L, Niu B, Zhu Z, Wu S, Li W. CD-HIT: accelerated for clustering the next-generation sequencing data. Bioinformatics. 2012;28(23):3150–2.
56. Nakashima K, Yamaguchi-Shinozaki K. ABA signaling in stress-response and seed development. Plant Cell Rep. 2013;32(7):959–70.
57. Rodríguez-Gacio MDC, Matilla-Vázquez MA, Matilla AJ. Seed dormancy and ABA signaling: the breakthrough goes on. Plant Signal Behav. 2009;4(11):1035–48.
58. Hasan MdM, Gong L, Nie ZF, Li FP, Ahammed GJ, Fang XW. ABA-induced stomatal movements in vascular plants during dehydration and rehydration. Environ Exp Bot. 2021;186:104436.
59. Bharath P, Gahir S, Raghavendra AS. Abscisic acid-induced stomatal closure: an important component of plant defense against abiotic and biotic stress. Front Plant Sci. 2021;12:615114.
60. Jin XF, Xiong AS, Peng RH, Liu JG, Gao F, Chen JM, et al. OsAREB1, an ABRE-binding protein responding to ABA and glucose, has multiple functions in Arabidopsis. BMB Rep. 2010;43(1):34–9.
61. Reinhart BJ, Weinstein EG, Rhoades MW, Bartel B, Bartel DP. MicroRNAs in plants. Genes Dev. 2002;16(13):1616–26.
62. Panjabi P, Jagannath A, Bisht NC, Padmaja KL, Sharma S, Gupta V, et al. Comparative mapping of Brassica juncea and Arabidopsis thaliana using Intron Polymorphism (IP) markers: homoeologous relationships, diversification and evolution of the A, B and C Brassica genomes. BMC Genomics. 2008;9(1):113.
63. Liu J, Rost B. Comparing function and structure between entire proteomes. Protein Sci. 2001;10(10):1970–9.
64. Rose A, Manikantan S, Schraegle SJ, Maloy MA, Stahlberg EA, Meier I. Genome-wide identification of arabidopsis coiled-coil proteins and establishment of the ARABI-COIL database. Plant Physiol. 2004;134(3):927–39.
65. Crick FHC. Is α-Keratin a coiled coil? Nature. 1952;170(4334):882–3.
66. Chen J, Li X, Ye X, Guo P, Hu Z, Qi G, et al. An S-ribonuclease binding protein EBS1 and brassinolide signaling are specifically required for Arabidopsis tolerance to bicarbonate. J Exp Bot. 2021;72(4):1449–59 Zhang J, editor.
67. Davletova S, Schlauch K, Coutu J, Mittler R. The Zinc-Finger protein Zat12 plays a central role in reactive oxygen and abiotic stress signaling in Arabidopsis. Plant Physiol. 2005;139(2):847–56.
68. Nishizawa A, Yabuta Y, Yoshida E, Maruta T, Yoshimura K, Shigeoka S. Arabidopsis heat shock transcription factor A2 as a key regulator in response to several types of environmental stress. Plant J. 2006;48(4):535–47.
69. Yang C, Guo W, Shi D. Physiological roles of organic acids in alkali-tolerance of the alkali-tolerant halophyte *Chloris virgata*. Agron J. 2010;102(4):1081–9.
70. Dornogovĭ, Mongolia Climate. Available from: https://weatherandclimate.com/mongolia/dornogovi
71. Mongolia - Climate Change and Disaster Risk Profile. Available from: https://www.unescap.org/sites/default/d8files/event-documents/Mongolia%20-%20Climate%20Change%20and%20Disaster%20Risk%20Profile.pdf
72. Jigjidsuren S, Johnson DA. Forage Plants in Mongolia. Ulaanbaatar: Admon printing; 2003.
73. Ngo TD, Krishnan M, Boutsalis P, Gill G, Preston C. Target-site mutations conferring resistance to glyphosate in feathertop Rhodes grass (*Chloris virgata*) populations in Australia. Pest Manag Sci. 2018;74(5):1094–100.
74. Mahajan G, Chauhan BS. Glyphosate efficacy in Chloris virgata Sw. in response to temperature and tank mixing. Plants. 2022;11(23):3190.
75. Zhong S, Chai H, Xu Y, Li Y, Ma JY, Sun W. Drought sensitivity of the carbon isotope composition of leaf dark-respired CO2 in C3 (Leymus chinensis) and C4 (Chloris virgata and Hemarthria altissima) Grasses in Northeast China. Front Plant Sci. 2017;8:1996.
76. Zhong S, Xu Y, Meng B, Loik ME, Ma JY, Sun W. Nitrogen addition increases the sensitivity of photosynthesis to drought and Re-watering differentially in C3 versus C4 grass species. Front Plant Sci. 2019;10:815.
77. Kim SJ, Na JU, Kim JS, Lee JE, Nie H, Lee KA, et al. Identification of valid reference genes for quantitative RT-PCR in Caragana microphylla under salt and drought stresses. Physiol Mol Biol Plants. 2020;26(10):2103–8.
78. Zhang TH, Su YZ, Cui JY, Zhang ZH, Chang XX. A Leguminous Shrub (Caragana microphylla) in Semiarid sandy soils of North China. Pedosphere. 2006;16(3):319–25.
79. Xiang DJ, Man LL, Cao S, Liu P, Li ZG, Wang XD. Heterologous expression of an Agropyron cristatum SnRK2 protein kinase gene (AcSnRK2.11) increases freezing tolerance in transgenic yeast and tobacco. 3 Biotech. 2020;10(5):209.
80. Bayat H, Nemati H, Tehranifar A, Gazanchian A. Screening different crested wheatgrass (Agropyron cristatum (L.) Gaertner.) accessions for drought stress tolerance. Arch Agron Soil Sci. 2016;62(6):769–80.
81. Nishiuchi S, Fujihara K, Liu S, Takano T. Analysis of expressed sequence tags from a NaHCO3-treated alkali-tolerant plant Chloris virgata. Plant Physiol Biochem. 2010;48(4):247–55.
82. Hereward JP, Werth JA, Thornby DF, Keenan M, Chauhan BS, Walter GH. Complete chloroplast genome sequences of two species of Chloris grass, Chloris truncata Sw. and Chloris virgata R.Br. Mitochondrial DNA Part B. 2016;1(1):960–1.
83. Mollard FPO, Di Bella CE, Loguzzo MB, Grimoldi AA, Striker GG. High recovery from either waterlogging or drought overrides any beneficial acclimation of chloris gayana facing a subsequent round of stress. Plants. 2022;11(20):2699.
84. Liphschitz N, Eshel AS, Waisel Y. Salt glands on leaves of Rhodes grass (Chloris gayana Kth). Ann Bot. 1974;38(2):459–62.
85. Kobayashi H, Masaoka Y, Takahashi Y, Ide Y, Sato S. Ability of salt glands in Rhodes grass (*Chloris gayana* Kunth) to secrete Na^+ and K^+. Soil Sci Plant Nutr. 2007;53(6):764–71.
86. Maybery-Reupert K, Isenegger D, Hayden M, Cogan N. Development of genomic resources for Rhodes grass (Chloris gayana), draft genome and annotated variant discovery. Front Plant Sci. 2023;14:1239290.
87. Lozano-Elena F, Fàbregas N, Coleto-Alcudia V, Caño-Delgado AI. Analysis of metabolic dynamics during drought stress in Arabidopsis plants. Sci Data. 2022;9(1):90.
88. Park SY, Jeong DH. Comprehensive analysis of rice seedling transcriptome during dehydration and rehydration. Int J Mol Sci. 2023;24(9):8439.

89. Zhou Y, Wang B, Yuan F. The role of transmembrane proteins in plant growth, development, and stress responses. Int J Mol Sci. 2022;23(21):13627.
90. Maurel C, Chrispeels MJ. Aquaporins. A molecular entry into plant water relations. Plant Physiol. 2001;125(1):135–8.
91. Yang SH, Kim SH, Berberich T, Kusano T. Identification and properties of a small protein that interacts with a tobacco bZIP-type transcription factor TBZF. Plant Biotechnol. 2012;29(4):395–9.
92. Lee HK, Cho SK, Son O, Xu Z, Hwang I, Kim WT. Drought stress-induced Rma1H1, a RING membrane-anchor E3 ubiquitin ligase homolog, regulates aquaporin levels via ubiquitination in transgenic *Arabidopsis* plants. Plant Cell. 2009;21(2):622–41.
93. Sun T, Ma N, Wang C, Fan H, Wang M, Zhang J, et al. A Golgi-Localized sodium/hydrogen exchanger positively regulates salt tolerance by maintaining higher K+/Na+ ratio in soybean. Front Plant Sci. 2021;12:638340.
94. Li M, Li Y, Li H, Wu G. Overexpression of AtNHX5 improves tolerance to both salt and drought stress in Broussonetia papyrifera (L.) Vent. Tree Physiol. 2011;31(3):349–57.
95. Munro S. The Golgin coiled-coil proteins of the Golgi apparatus. Cold Spring Harb Perspect Biol. 2011;3(6):a005256–a005256.
96. Malsam J, Satoh A, Pelletier L, Warren G. Golgin tethers define subpopulations of COPI vesicles. Science. 2005;307(5712):1095–8.
97. Seemann J, Jokitalo E, Pypaert M, Warren G. Matrix proteins can generate the higher order architecture of the Golgi apparatus. Nature. 2000;407(6807):1022–6.
98. Latijnhouwers M, Gillespie T, Boevink P, Kriechbaumer V, Hawes C, Carvalho CM. Localization and domain characterization of Arabidopsis golgin candidates. J Exp Bot. 2007;58(15–16):4373–86.
99. Nisa ZU, Mallano AI, Yu Y, Chen C, Duan X, Amanullah S, et al. GsSNAP33, a novel Glycine soja SNAP25-type protein gene: Improvement of plant salt and drought tolerances in transgenic Arabidopsis thaliana. Plant Physiol Biochem PPB. 2017;119:9–20.

Publisher's Note